

Addressing Barriers to Efficient Renewable Integration

Milestone Report 1

Lead organisation: University of New South Wales (UNSW)

Project Partners: AEMO, ElectraNet, TasNetworks

Project Commencement Date: 02 July 2018

Project Completion Date: 02 July 2021

Authors: Shabir Ahmadyar, Leonardo Callegaro, Christian Rojas Monrroy, Georgios Konstantinou, Jenny Riesz, John Fletcher

Contact Name: John Fletcher

Title: Professor, School of Electrical Engineering and Telecommunication

Email: john.fletcher@unsw.edu.au

Date: 21 February 2019

Project Information: <https://arena.gov.au/projects/addressing-barriers-efficient-renewable-integration/>

Inverter Bench Testing Results: <http://pvinverters.ee.unsw.edu.au>

This activity received funding from *Australian Renewable Energy Agency (ARENA)* as part of *ARENA's Emerging Renewables Programme*. The views expressed herein are not necessarily the views of the Australian Government, and the Australian Government does not accept responsibility for any information or advice contained herein.

EXECUTIVE SUMMARY

This technical report presents the details and findings for the project "Addressing barriers to efficient integration of renewables", for the period 02 Jul 2018 to 05 Jan 2019. The specific topics discussed in this report include:

- Task 1** Bench tests of common PV inverters with a wide range of voltage and frequency disturbances based on AS4777.2-2015.
- Task 2** Collect and analyse measured data for different frequency and voltage disturbances to serve as a basis for the DER as well as composite load modelling.
- Task 3** Development of DER model, including tuning and model validation of the DER_A parameters based on the findings from Task 1 and Task 2.

The main findings and conclusions from the work completed are as follows:

1. The PV inverters bench testing demonstrated that inverters' responses to the same disturbance are diverse and different from a system dynamic point of view. This difference can, consequently, impact the modelling and aggregation of DERs for bulk power system (BPS) studies, and also have a detrimental effect on the grid by causing large reductions in the generation as a result of the inverter responses. *This is shown in Chapter 2.*
2. A set of voltage and frequency disturbances has been analysed using PMU and high-speed PQM data. Possible DER trip events have been observed, which can be confirmed after obtaining more information from the monitored feeders, e.g., load composition, voltage control strategy, etc. One of the main challenges is to discern between the voltage and frequency dependency of the traditional loads and the response of DERs to voltage and frequency disturbances. Hence, in addition to the DER modelling, it is very important to present dynamics of the load accurately by considering correct load composition. *See Chapter 3 for details.*
3. This subtask utilises the DER_A model that was recently developed by the Western Electricity Coordinating Council (WECC) to represent dynamics of DER for BPS studies [1]. This model mimics the aggregated behaviour of inverter-based DERs on a load bus for voltage and frequency disturbances. The model is generic and can be parameterised for different DERs' settings. Based on the findings from Task 1 and Task 2, as well as the requirements set at AS4777.3-2005 and AS4777.2-2015, the parameters are tuned for voltage and frequency disturbance. *See Chapter 4 for more details.*

Abbreviations and Acronyms

AEMO	Australian Energy Market Operator
ARENA	Australian Renewable Energy Agency
AS	Australian standards
BPS	Bulk power system
CEC	Clean Energy Council of Australia
DERs	Distributed energy resources
EMT	Electromagnetic Transient
HVRT	High voltage ride through
LVRT	Low voltage ride through
NEM	Australian national electricity market
PMU	Phasor measurement unit
PV	Photovoltaics
POI	Point of interconnection
PQM	Power quality meter
PSSE	Power system simulator for engineering, RMS simulation tool.
RMS	Root mean square
RoCoF	The rate of change of frequency
SMIB	Single machine infinite bus
UNSW	The University New South Wales
WECC	Western Electricity Coordinating Council

CONTENTS

EXECUTIVE SUMMARY	1
Abbreviations and Acronyms	2
CONTENTS	3
LIST OF FIGURES	5
LIST OF TABLES	7
1 Introduction	8
1.1 Scope of deliverable	8
1.2 Methodology for DER modelling	9
2 Inverter bench testing	11
2.1 Summary	11
2.1.1 Highlights so far – AS4777.2 non-compliance and detrimental responses	11
2.2 Methodology	12
2.3 Preliminary results	15
2.3.1 Frequency steps within the limits of AS/NZS 4777.2:2015	16
2.3.2 Response to grid voltage phase angle change	18
2.3.3 Additional tests highlighting differences between inverter behaviours.....	22
2.4 Future works	22
3 Data collection and analyses for DER and load modelling	23
3.1 Voltage Disturbances	23
3.1.1 Australian standards	23
3.1.2 Energy Queensland data - Currimundi feeder	24
3.1.3 Summary	27
3.2 Frequency Disturbances	27
3.2.1 Australian standards	27
3.2.2 Frequency trip settings	28

3.2.3	TasNetworks data – Kingston feeder	30
4	DER model development	35
4.1	International work	35
4.2	DER parameters per AS4777	38
4.3	Time domain simulations	42
4.3.1	Voltage disturbances	42
4.3.2	Frequency disturbances	47
4.4	Summary	49
5	Conclusions	50
6	References	51

LIST OF FIGURES

Figure 1: DER model development methodology	9
Figure 2: Schematic representation of the bench testing setup.	13
Figure 3: Inverter bench-testing laboratory setup.	13
Figure 4: Electrical characteristics of the solar array emulator.	13
Figure 5: Example of test programmed in the grid emulator control interface.	14
Figure 6: Example of plot resulting from post-processing analysis of the measured data showing grid voltage and current, PV voltage and current, and post-processed real and reactive power.	15
Figure 7: Expected frequency response curve for the PV inverter [3, p. 31].	16
Figure 8: Results following a step in the frequency in the grid voltage from 50 to 51.95 Hz. (From top to bottom: INV#1, #2 and #3).	17
Figure 9: Results following a step in the frequency in the grid voltage from 50 to 47.05 Hz. (From top to bottom: INV#1, #2 and #3).	18
Figure 10: Phase-jump test profile programmed in the grid emulator.	19
Figure 11: Results following 15° voltage phase angle change in the grid voltage. (From top to bottom: INV#1, #2 and #3).	20
Figure 12: Results following 30° voltage phase angle change in the grid voltage. (From top to bottom: INV#1, #2 and #3).	21
Figure 13: Event 1 – 0.84 pu asymmetrical fault measured at Currimundi (Wednesday 15 th February 2017, 10:34 am), active power and voltage.	25
Figure 14: Event 1 – 0.84 pu asymmetrical fault measured at Currimundi (15th February 2017, 10:34 am), instantaneous voltage and current for phase C.	26
Figure 15: Event 1 – 0.84 pu asymmetrical fault measured at Currimundi (15th February 2017, 10:34 am), the instantaneous voltage for all phases.	26
Figure 16: Event II – 25 August 2018, 1:11 pm	32
Figure 17: Event II – 25 August 2018, 1:11 pm, all channels	33
Figure 18: Composite Load Model with Distributed Generation (DG).	36
Figure 19: proposed DER_A model [1].	37
Figure 20: Proposed composite load and DER model, based on the WECC model.	38
Figure 21: Single line diagram of the SMIB model in PSSE	42
Figure 22: DER_A response to 0.7 pu voltage disturbance for 1 sec.	43
Figure 23: DER_A response to 0.7 pu voltage disturbance for 1.5 sec.	43
Figure 24: DER_A response to 0.7 pu voltage disturbance for 2 sec.	44
Figure 25: Effect of Vfrac on partial tripping of DER.	44
Figure 26: DER_A response to 0.8 pu voltage disturbance for 2 sec.	45
Figure 27: DER_A response to 0.9 pu voltage disturbance for 8 sec.	45
Figure 28: DER_A response to 1.13 pu voltage disturbance for 8 sec.	46
Figure 29: DER_A response to 1.2 pu voltage disturbance for 2 sec.	46
Figure 30: DER_A response to 46.94 Hz frequency disturbance for 1.8 sec.	47
Figure 31: DER_A response to 46.94 Hz frequency disturbance for 1.4 sec.	47

Figure 32: DER_A response to 47.02 Hz frequency disturbance for 7.25 sec.....	48
Figure 33: DER_A response to 51.98 Hz frequency disturbance for 7.25 sec.....	48
Figure 34: DER_A response to 52.02 Hz frequency disturbance for 0.08 sec.....	48
Figure 35: DER_A response to 52.02 Hz frequency disturbance for 0.2 sec.....	49

LIST OF TABLES

Table 1: Location of PMUs and high-speed PQMs.....	23
Table 2: Voltage set-point values defined in AS4777.2-2015.	24
Table 3: Voltage set-point values defined in AS4777.3-2005.	24
Table 4: Currimundi feeder voltage disturbance events summary.....	25
Table 5: Frequency set-point values defined in AS4777.2-2015.	28
Table 6: Frequency set-point values defined in AS4777.3-2005.	28
Table 7: Frequency trip settings of distributed PV for under-frequency events (as of May 2015).....	29
Table 8: Frequency trip settings of distributed PV for over-frequency events (as of May 2015).....	30
Table 9: Kingston feeder frequency disturbance summary.....	31
Table 10: Proportion of PV installation according to different standards (as at Sept 2018).	37
Table 11: DER parameters per AS4777	38

1 Introduction

Reliable and economic integration of distributed energy resources (DERs), such as rooftop photovoltaics (PV) and storage introduces specific challenges resulting from their widespread growth. Higher penetration of DERs not only impact the steady state but also the dynamic performance of the bulk power system (BPS). Hence, efficient integration of DERs necessitates continued improvements in forecasting, modelling and improved interconnection requirements. This can, consequently, improve overall system performance.

In recent years, the penetration of DERs in the Australian national electricity market (NEM) has increased significantly. Considering this, it is crucial to develop accurate DER models for BPS studies. To partially address this, the Australian Renewable Energy Agency (ARENA) under the Emerging Renewables Program has funded this project to develop accurate DER models. The aim of this project is to develop generic DER and composite load models that can be used for RMS studies in BPS.

1.1 Scope of deliverable

This deliverable (milestone report 1) presents the findings based on Task 1 and Task 2. The goals of this report are as follows:

Task 1: Bench testing of commonly used PV inverters for a wide range of voltage and frequency disturbances based on AS4777.2-2015.

See Chapters 2.

This subtask deals with the bench testing of PV inverters. A short list of commonly used inverters in Australia has been prepared. A selected number of these inverters have been tested with disturbances and their performance has been documented. The inverter behaviour will inform the DER model development and other applications. Examples of inverter tests include:

- Response to frequency deviation within the limits of AS 4777.2-2015 (i.e., $47 \text{ Hz} < f < 52 \text{ Hz}$).
- Response to high RoCoF, with frequency boundary within the limits of AS 4777.2– 2015.
- Response to grid voltage phase angle change.
- Response to short duration grid voltage sags.

Task 2: Collect and analyse measured data for different frequency and voltage disturbances to serve as a basis for the DER as well as composite load modelling.

See Chapter 3 for details.

This subtask attempts to collect measured data from phasor measurement units (PMU) as well as power quality metres (PQMs) aiming to capture and model the aggregated behaviour of DERs and loads considering daily/seasonal variations. So far, measured data from four feeders in Queensland and one feeder in Tasmania have been analysed and some conclusions have been made.

Task 3: Development of DER model, i.e., tuning and model validation of the DER_A parameters based on the findings from Task 1 and Task 2.

See Chapter 3 for details.

This subtask utilises the DER_A model that was recently developed by the Western Electricity Coordinating Council (WECC) to represent dynamics of DER for BPS studies [1]. This model mimics the aggregated behaviour of inverter-based DERs on a load bus for voltage and frequency disturbances. The model is generic and can be parameterised for different DERs' settings. Based on the findings from Task 1 and Task 2, as well as the requirements set at AS4777.3-2005 and AS4777.2-2015, the parameters are tuned for voltage and frequency disturbance.

1.2 Methodology for DER modelling

This section briefly describes the methodology for the development of DER model for BPS studies, as illustrated in Figure 1.

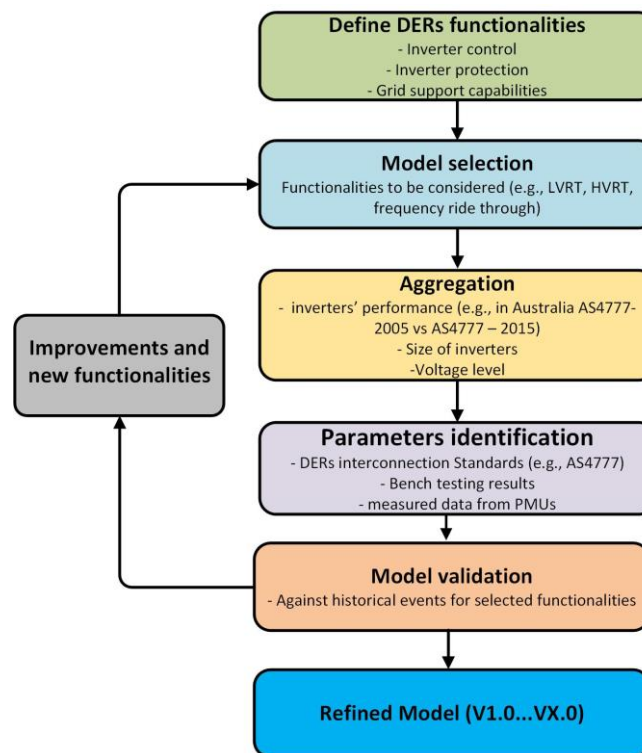


Figure 1: DER model development methodology

1. **Define DERs functionalities:** The inverter manufacturers usually set these functionalities according to the grid code requirements, e.g., AS4777.2 - 2015 in Australia, for volt-var, volt-watt, LVRT, HVRT and other requirements.
2. **Model selection:** Considering the DER functionalities, a suitable RMS type DER model is selected, i.e., DER_A [1]. Note that the model is generic, which aggregates the DERs in a single load/DER bus. The importance of generic (or aggregated) load/DER modelling for power system studies (e.g. stability, security and protection analysis) has been acknowledged by the research community as well as the industry [2]. A key feature of generic models is that they do not depend on practical details which will vary in the long-term. In other words, this implies that generic models aim to represent the common behaviour of millions

of customers instead of modelling particular physical loads/DERs with their specific details. This concept is already well-known in power systems. For instance, conventional generic load models represent the aggregated effect of millions of devices by simple analytical expressions. Note that generic models are used in large numbers of case and scenario studies. Therefore, with respect to the trade-off between accuracy and computational speed, they demand some simplifications.

3. **Aggregation:** as discussed above, the DERs will be clustered according to their performance, e.g., in Australia inverters installed prior to October 2016 likely to comply with AS4777.3-2005; whereas, those installed post October 2016 likely comply with AS4777.2-2015. Hence, their performance will be different, which should be considered while aggregating. Other factors that impact the aggregation would be the point of connection, i.e., at which voltage level are they connected.
4. **Parameters identification:** the DER_A model has the capability to accommodate the frequency and voltage ride through requirements set in AS4777.3-2005 as well as AS4777.2-2015. Hence, the requirements set on those standards as well as inverters' bench testing results and measured data from real disturbances in the grid will be used to identify the aggregated parameters of DERs.
5. **Model validation:** once the parameters are identified, a set of standard disturbances based on the historical events on the monitored feeders will be applied to compare the performance of the model with the physical devices. To do this, a single machine infinite bus (SMIB) model of the monitored feeders will be used. To ensure the accuracy, it is important to have a realistic composite load model representing the voltage and frequency dependency as well as the voltage recovery behaviour of the load and distinguishing between to load response and the DER response.
6. **Refined mode:** the first version of the model will be available for BPS studies. However, as more data becomes available, the DER_A model parameters can be further tuned and/or more functionalities can be added. Note that load/DER modelling is an iterative task and as the grid evolve, the system operators should ensure that the model is up-to-date and represents the current status.

2 Inverter bench testing

Creation of a DER model for PV inverters requires an understanding of the behaviour of the inverters when these are subjected to voltage and frequency disturbances. The connection between the grid voltage and frequency variations with the active and reactive power delivered by the inverter is fundamental to developing a useful DER model.

The scope of the bench testing is to observe the response of commercial PV inverters under different types of grid disturbances. The motivation of the bench testing is:

- To utilise these results to assist in the development of a DER model.
- To assess whether inverters are 'robust' to grid disturbances.
- To benchmark the inverters against the standard enforced at the time.
- To identify possible enhancements to future standards.
- To attempt to confirm/refute common perceptions around small-scale inverters.

Observing the response of the inverter in terms of active and reactive power, when the grid voltage and frequency are varied according to specific patterns is the tool which is used to infer the dynamic behaviour of the inverters and for creating a DER model.

2.1 Summary

The Australian Standard AS4777.2-2015: '*Grid connection of energy systems via inverters - Inverter requirements* [3]' specifies requirements and tests for low voltage inverters for the injection of electric power through an electrical installation into the grid at low voltage [3]. Many of the tests carried out in the bench testing procedure are inspired by clauses taken from [3]. However, the bench testing is not intended to verify the inverter compliance to the standard itself, but rather to identify and benchmark inverters' behaviour when subjected to grid disturbances.

So far, we have tested five inverters, named here as INV#1 to INV#5. The choice of inverters was based on the following analysis of the register of systems:

- **INV#1:** A 5kW inverter whose combined capacity represents 240MW of inverter connected generation in the NEM.
- **INV#1 to #5:** represent around 10.5 % of the inverter capacity installed for rooftop PV systems in the NEM. This is 140,000 inverters with a rated power of 700 MW.
- Each inverter represents 1-3.5% of market share. The combined market share of the 5 inverter manufacturers is around 30%: equivalent to 1.8-2.0 GW.

2.1.1 Highlights so far – AS4777.2 non-compliance and detrimental responses

Behaviour 1: INV#1, #2 and #4 (representing 500MW) reduce power injection to zero with a voltage phase angle change of greater than 30°. Recovery time, 7 mins. Voltage phase angle change might be the outcome of line switching or asymmetric faults. The potential impact is a large-scale disconnection of inverter types #1, #2 and #4.

Behaviour 2: INV#2 and #5 (representing 250MW of generation) failed the fast voltage sag test. This would result in these two inverter types disconnecting during a short duration voltage sag and the loss of up to 250MW of generation. Recovery time, 7 mins.

Behaviour 3: INV#2 and #4 trip too quickly on under frequency. They cannot contribute active power during an under frequency event and will cause the rapid loss of up to 280MW of generation. Recovery time, 7 mins.

Behaviour 4: Volt-Watt response: only one inverter performed this function correctly (INV#2). The other inverters' Volt-Watt response was either too slow or resulted in a disconnect (representing 610 MW of lost generation).

Behaviour 5: INV#5 (representing 70 MW) will not tolerate a RoCoF above 0.4 Hz/s. With a RoCoF above this level, INV#5 will disconnect exacerbating the initial cause of the high RoCoF. Recovery time, 7 mins.

Behaviour 6: INV#3 responds slowly to an over-frequency, so slow that it could be ignored as a source of generation relief in the network. This represents 120MW of generation that continues to be injected when it should not.

All of the above represent challenges for the network in the present day. As installations continue at a rapid pace, it is essential to evolve and tighten the standards in force as these issues will be further compounded with large-scale aggregation and virtual power plant business models.

In the following sections, the methodology used for bench-testing inverters is described. Afterwards, some key results from the first set of tests are reported. These identify inverters' behaviours under selected grid frequency and voltage disturbances. Finally, the main observations from the first round of bench-testing are gathered and directions for future research are given.

2.2 Methodology

The setup for the inverter bench testing is composed of the PV inverter, a PV emulator (on the right of Figure 2), and a grid emulator (on the left of Figure 2). The PV emulator produces DC electrical power, which is converted by the PV inverter into AC power and delivered to the grid (using a grid emulator).

The schematic in Figure 2 is implemented in the laboratory, where instrumentation is added to monitor the waveforms of voltage, current and power of interest. The laboratory setup is displayed in Figure 3.

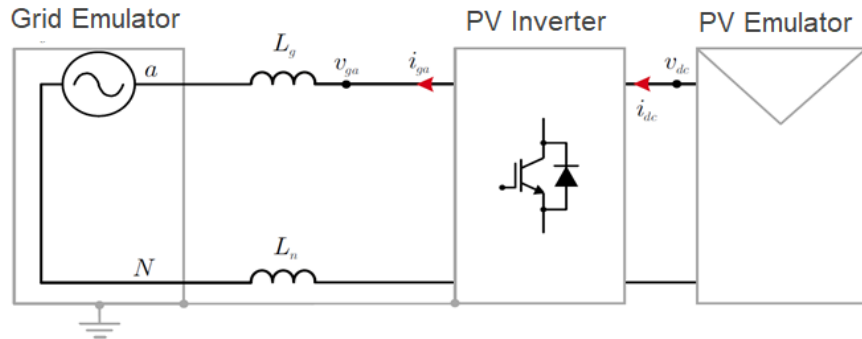


Figure 2: Schematic representation of the bench testing setup.

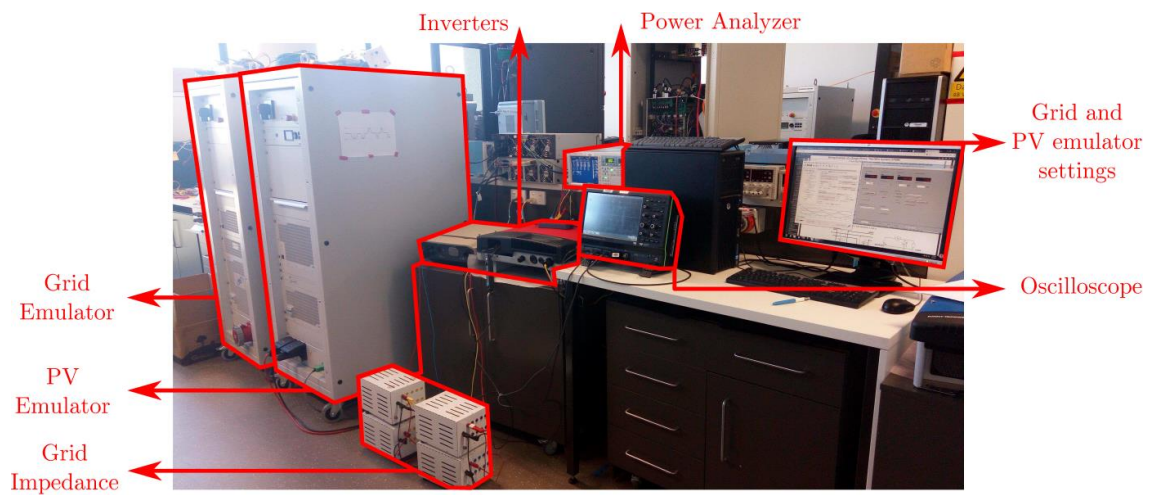


Figure 3: Inverter bench-testing laboratory setup.

The PV emulator provides power to the inverter, according to the characteristic of a 4.6 kW solar array, represented in Figure 4.

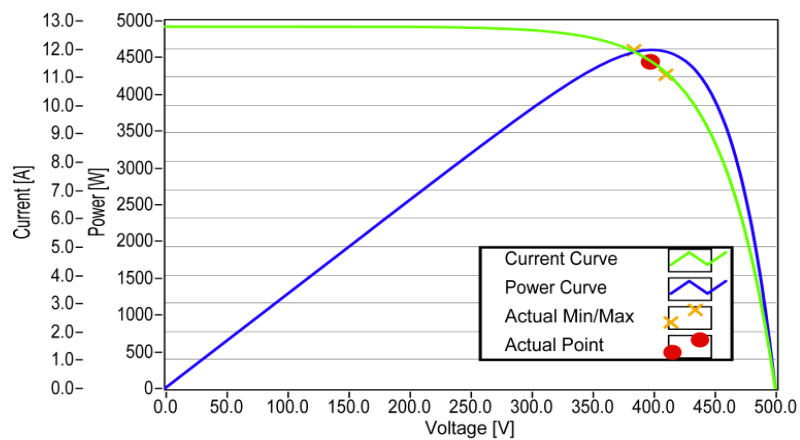


Figure 4: Electrical characteristics of the solar array emulator.

Note the red circle in Figure 4, showing the operating point of the inverter in the *current-voltage* characteristic (in green), and corresponding to the maximum power point of the (blue) parabola, representing the *power – voltage* characteristic of the solar array.

While the input side of the inverter operates at the quiescent point specified in Figure 4, the output is feeding power to the grid emulator, which represents the 230 V, 50 Hz grid. The grid emulator and the PV inverter are separated by an interfacing inductance, whose value is chosen according to [3]. The grid emulator is programmed to change parameters of the grid voltage, such as voltage amplitude, frequency, phase angle and so on, according to the tests specified in the procedure used for the bench testing. Figure 5 represents an example of a test profile programmed in the grid emulator.

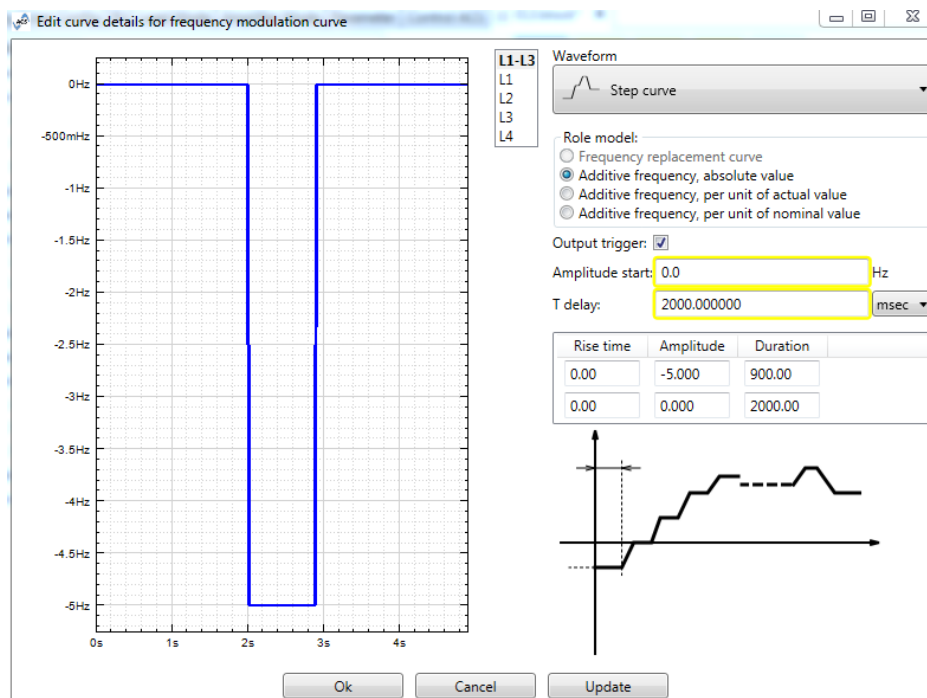


Figure 5: Example of test programmed in the grid emulator control interface.

In the test specified in Figure 5, the frequency of the grid is programmed to decrease by 5 Hz, going from an absolute value of 50 Hz to 45 Hz, for a time duration of 2 s. Following the disturbance imposed by the grid emulator, the values of voltage and current at the input and at the output of the PV inverter are recorded, by means of a digital oscilloscope. Post-processing the data helps interpret the behaviour of active and reactive power delivered by the PV inverter to the grid emulator. An example of a plot resulting from post-processing analysis is displayed in Figure 6.

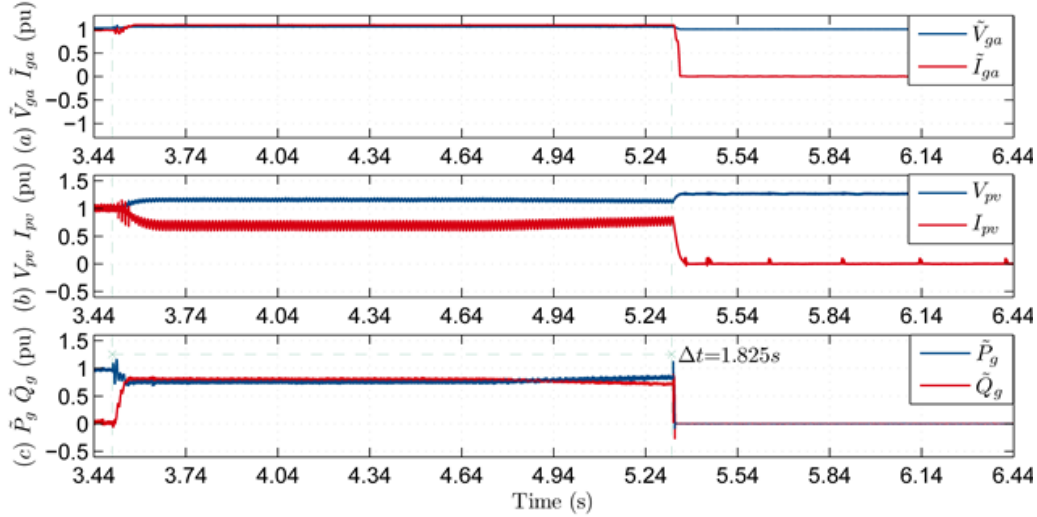


Figure 6: Example of plot resulting from post-processing analysis of the measured data showing grid voltage and current, PV voltage and current, and post-processed real and reactive power.

The plot in Figure 6 results from the test displayed in Figure 5, where the grid frequency is decreased from 50 Hz to 45 Hz, for 2 s. The top sub-plot in Figure 6 displays the AC voltage (\tilde{V}_{ga}) and current (\tilde{I}_{ga}) at the inverter AC output port, the middle sub-plot shows the voltage (V_{pv}) and current (I_{pv}) at the output of the PV emulator, and the bottom subplot shows the active (\tilde{P}_g) and reactive power (\tilde{Q}_g) delivered by the inverter to the grid, all values are in per unit. It is noticeable that the negative 5 Hz frequency excursion causes the inverter to disconnect (after 1.825 s at $t = 5.24$ s time-mark in Figure 6). Furthermore, the disconnection occurs in less than 2 s, as demanded by [3, p. 29].

2.3 Preliminary results

A detailed testing procedure specifying 43 different tests has been developed, see https://unsw-my.sharepoint.com/:f/g/personal/z5030488_ad_unsw_edu_au/EpxGgsjvBRKnjKF4Wkg5OcBYyganacCQ9poN-f-TpAwnw?e=dj137y. This procedure divides the tests into groups according to the variable which is being perturbed.

- *Steady-state performance* tests aim to verify the inverter behaviour when all quantities are in the steady-state state, for a solar irradiation value of 1000 W/m² and 500 W/m², at which the inverter delivers full or half of its rated power to the grid emulator, respectively.
- *Power dynamic response* tests verify the inverter behaviour for different solar irradiation profiles.
- *Frequency response* and *voltage response* tests verify the behaviour of the inverter when the frequency or the amplitude of the grid voltage is being varied, respectively.
- *Reconnection behaviour* tests verify that the inverter complies with the minimum reconnection time after a voltage or frequency variation event, beyond the limits specified in [3].
- *Voltage phase angle change* tests verify the dynamic behaviour of the inverter when the grid voltage phase angle is abruptly changed.
- *Efficiency* tests aim to measure the inverter efficiency for different operating power levels.

So far, five PV inverters have been tested in the laboratory as reported in Section 2.1. The inverters tested are among the most popular brands used in Australia for connection of domestic PV systems to the low voltage AC grid. The results collected permitted to highlight some key differences between inverters. The next paragraphs summarise the main observations from the first set of tests for three of those inverters (INV#1-3).

2.3.1 Frequency steps within the limits of AS/NZS 4777.2:2015

These tests are related to the *frequency response* category, and verify the behaviour of inverters in the following circumstance:

- Grid frequency step from 50 to 51.95 Hz
- Grid frequency step from 50 to 47.05 Hz

It is expected that the inverters keep operating connected to the AC grid in either case¹ and vary the value of the active power according to the curve reported in [3, p. 31], represented again in Figure 7.

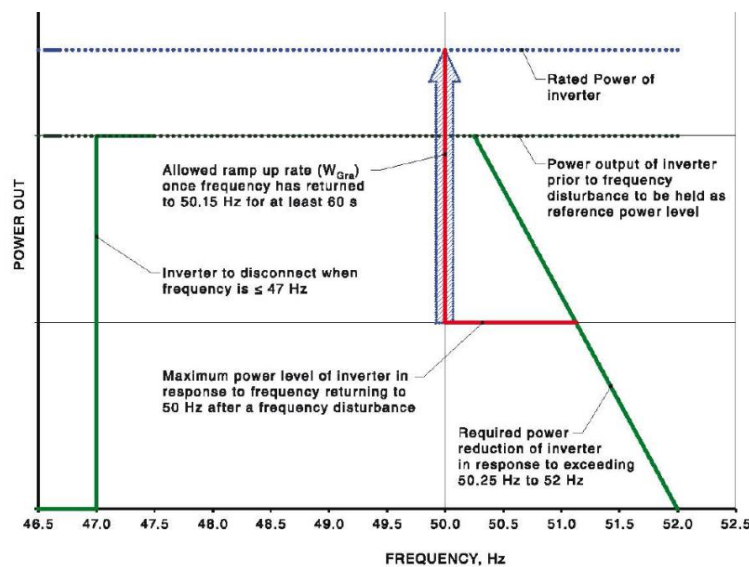


Figure 7: Expected frequency response curve for the PV inverter [3, p. 31].

The post-processed plots for the first case (step from 50 to 51.95 Hz) are displayed in Figure 8 (from the top to the bottom, sub-plot for INV#1 to INV#3, respectively). In all cases displayed in Figure 8, each inverter reduces the output active power (blue curve in the bottom graph of each sub-plot), after the grid frequency is stepped from 50 to 51.95 Hz at the 3.5 s time mark, in accordance with the requirement specified in *clause 7.5.3.1 'Response to an increase in frequency'* of [3, pp. 29-31]. However, it is noticeable that the time taken by each inverter to reduce the active power delivered is very different. INV#1 and INV#2 reduce the active power in less than 1 s, while INV#3 takes well above 10 s to reduce the active power output.

¹ Inverters should remain online for these frequencies. However, they might trip because of high RoCoF (step change in frequency corresponds to a very high RoCoF ≈ 1000).

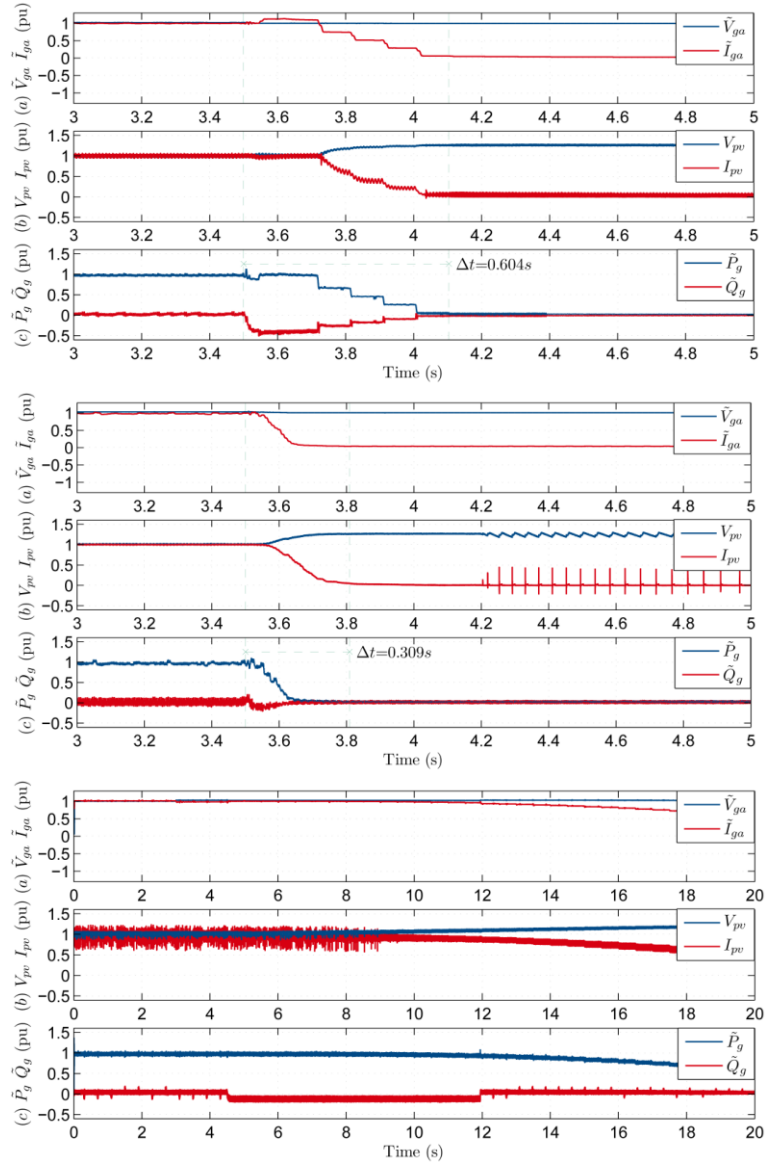


Figure 8: Results following a step in the frequency in the grid voltage from 50 to 51.95 Hz. (From top to bottom: INV#1, #2 and #3).

The plots for the second case (step from 50 to 47.05 Hz) are displayed in Figure 9, confirming that the active power delivered by the inverter is not diminished when the frequency is decreased and kept higher than 47 Hz, in accordance with Figure 7. However, it is interesting to observe the momentary variation in the reactive power, after the step in frequency is applied at the 3.5 s time mark. While for INV#2 the reactive power transient following the decrease in the frequency lasts for a few hundred ms, for INV#1 and INV#3 the reactive power transient takes several seconds before settling.

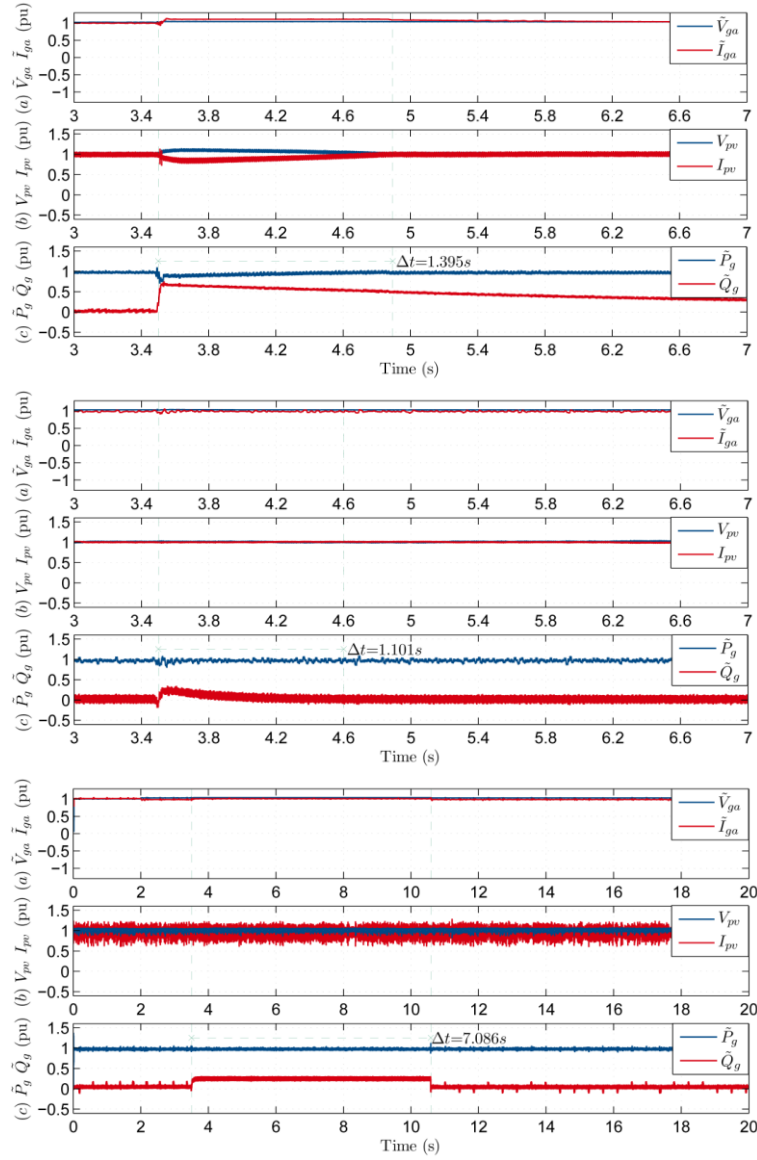


Figure 9: Results following a step in the frequency in the grid voltage from 50 to 47.05 Hz. (From top to bottom: INV#1, #2 and #3).

2.3.2 Response to grid voltage phase angle change

The response to grid voltage phase angle change highlighted again very different behaviour among inverters from different manufacturers. Furthermore, learnings from the results reported in Section 2.3.1 can be used to infer some preliminary conclusions. In these tests, the phase angle of the grid voltage is stepped by 15° and 30° , with the pattern specified in Figure 10. Note that the phase angle is varied and maintained at the new value for 2 s, and afterwards is brought back to zero.

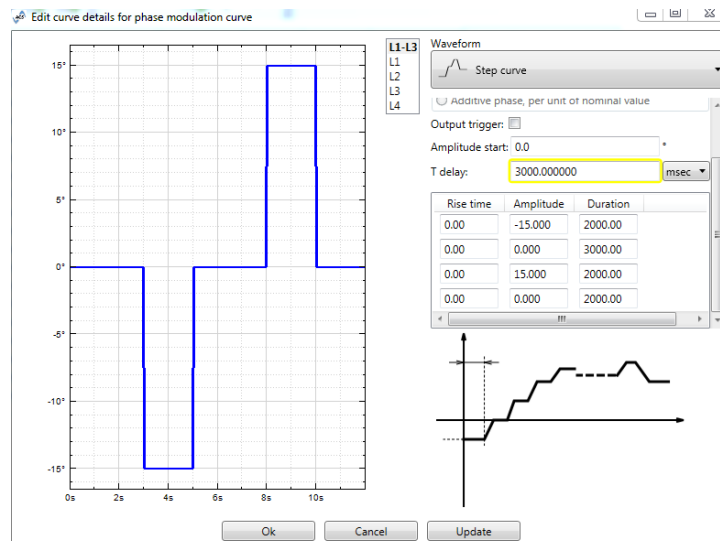


Figure 10: Phase-jump test profile programmed in the grid emulator.

Figure 11 presents the results following a positive 15° voltage angle change, occurring at 4.5 s time mark. The phase angle change causes a temporary loss of synchronism between the inverter AC voltage (\tilde{V}_{ga} , blue waveform) and AC current (\tilde{I}_{ga} , red waveform) as visible in the first graph of each sub-plot. As a result, active power (\tilde{P}_g) and reactive power (\tilde{Q}_g) delivered by each inverter undergo a transient, visible in the bottom graph of each sub-plot. The AC current of INV#1 and INV#2 takes at least one or two AC cycles to return in phase with the inverter voltage. A loss of synchronism between the AC current and voltage of INV#3 appears instead less obvious, and so do the variation of active and reactive power in the same inverter. This is in accordance with the observations following the response to a frequency step from 50 to 51.95 Hz, in Section 2.3.1, where INV#3 showed a response time greater than 10 s. It is concluded that since the 15° phase angle change only lasts a few cycles, and INV#3 takes tens of seconds to react, the phase angle change does not significantly vary the operation of this inverter.

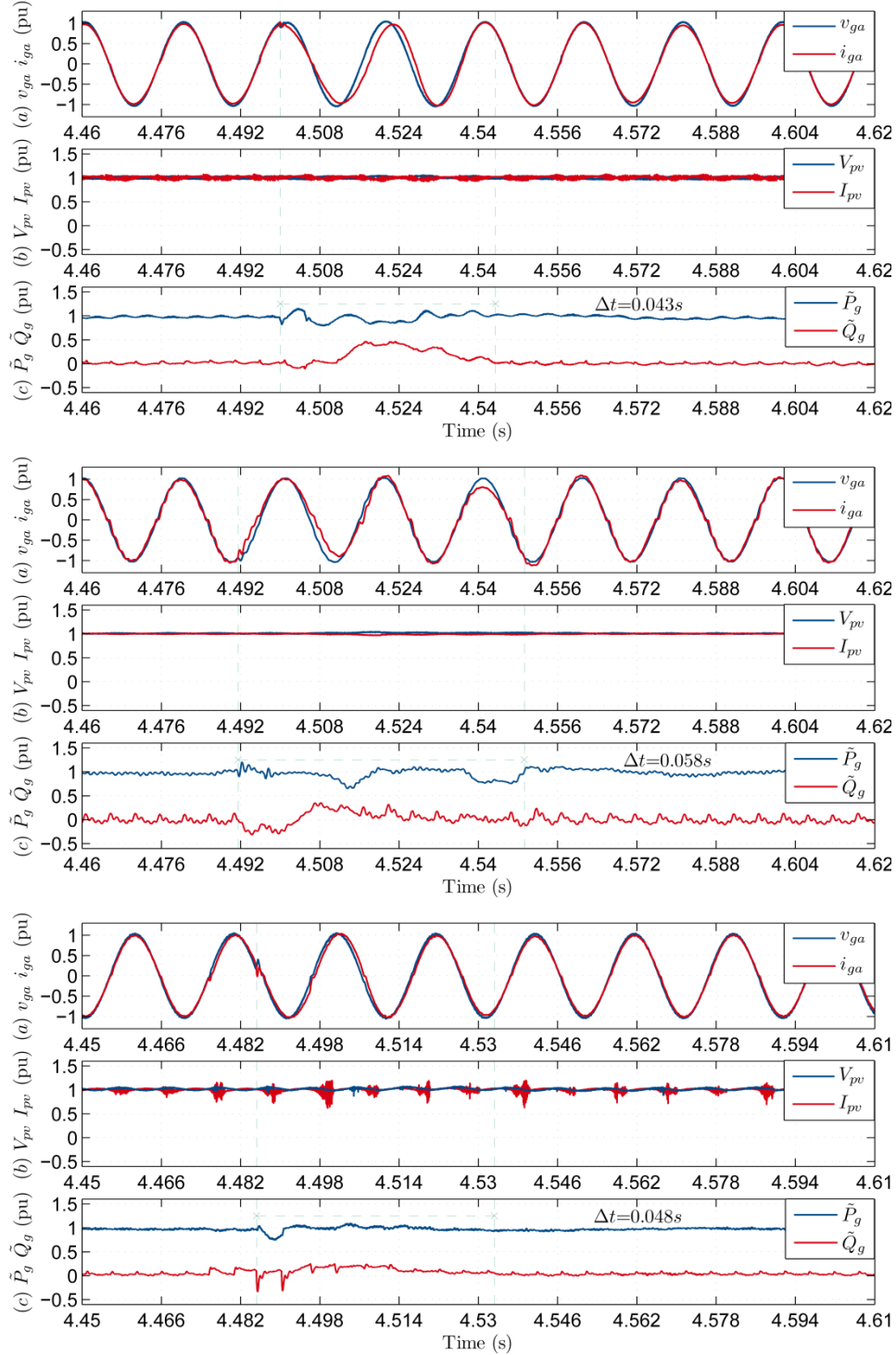


Figure 11: Results following 15° voltage phase angle change in the grid voltage. (From top to bottom: INV#1, #2 and #3).

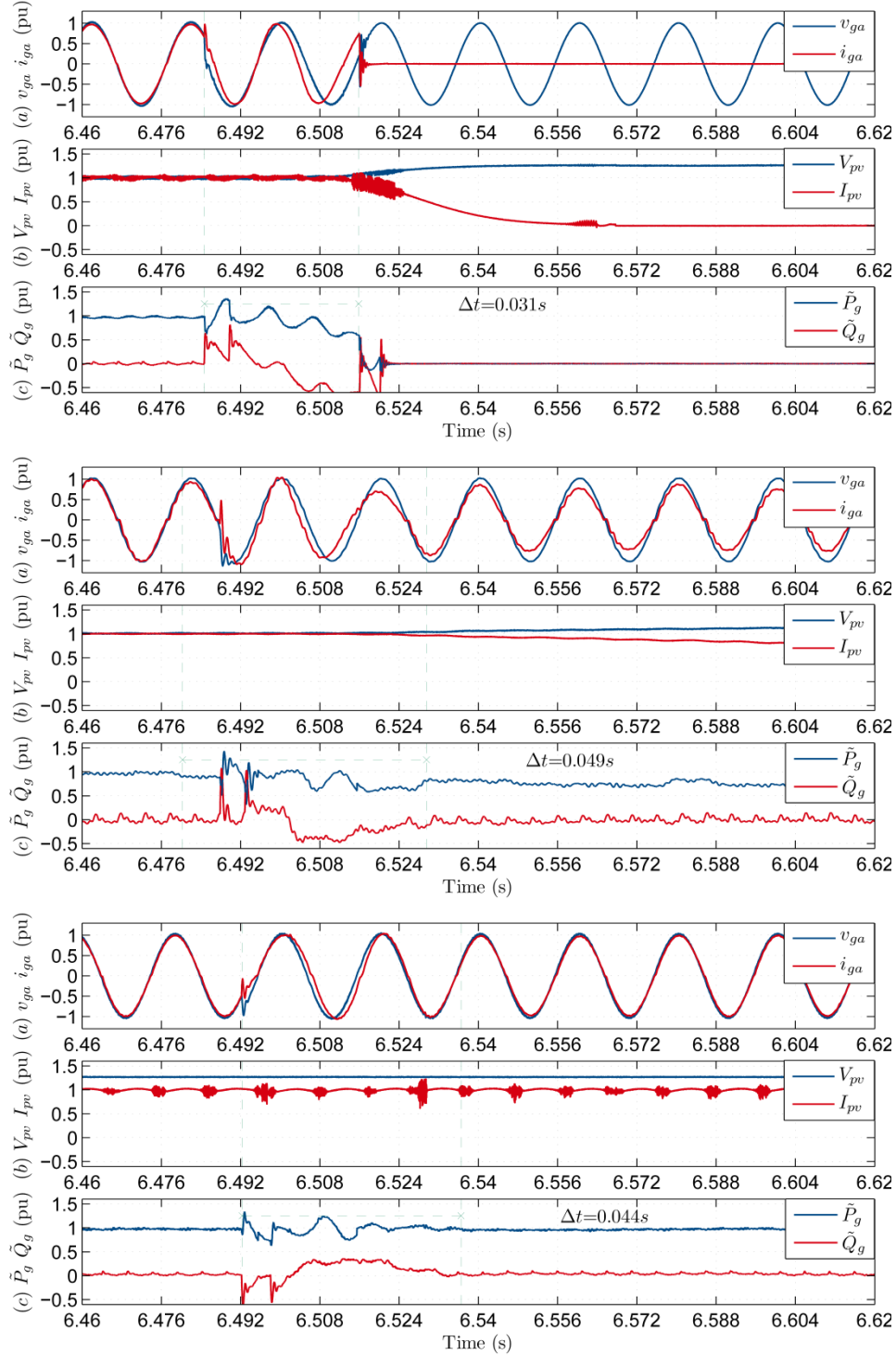


Figure 12: Results following 30° voltage phase angle change in the grid voltage. (From top to bottom: INV#1, #2 and #3).

Figure 12 shows response of inverters to a positive 30° voltage phase angle change. INV#1 loses synchronism between the AC voltage and current, and eventually disconnects indicating a grid over-frequency alarm. With INV#2, the grid current is re-synchronised to the voltage within two AC cycles. However, the active power following the phase angle change is decreased compared to the active power prior to the disturbance. This is also apparent from the waveform of the grid current, whose peak after the phase angle change is lower than before the disturbance. In the case of INV#2, it seems that the phase angle change is interpreted by the control system like an over-frequency event, below the disconnection threshold of Figure 7, such that the active power delivered by the inverter is decreased. In the case of INV#3, the phase angle change causes a temporary loss of synchronism, which is recovered within one ac cycle. Also, in the case of Figure 12, INV#3 is less sensitive to phase angle change compared to INV#1 and INV#2, and this is attributed to the slow response to frequency changes shown by INV#3.

2.3.3 Additional tests highlighting differences between inverter behaviours

Section 2.3.1 and Section 2.3.2 pointed out the different behaviour of the inverters tested under frequency steps and voltage phase angle change. Other significant tests and their results are reported in a power point presentation which was delivered to the steering committee and the industry advisory group. The additional results can be seen at: <http://pvinverters.ee.unsw.edu.au/>.

2.4 Future works

In the next stage of the project, more inverters will be subjected to the bench testing procedure, with the scope of benchmarking behaviours caused by disturbances in the grid voltage. The focus remains on those tests analysing the behaviour of the PV inverters following voltage or frequency disturbances in the AC grid voltage. Furthermore, the inverters tested so far were declared compliant to [3] by their manufacturers. In the next part of the project, inverters complying with [3] as well as with a 2005 version of the same standard, [4], will be tested. This will allow gaining more knowledge regarding the behaviour of PV inverters installed in Australia and possibly lead to the creation of two DER models, one for inverters complying with [3] and one for inverters complying with [4].

3 Data collection and analyses for DER and load modelling

The aim of this Subtask is to collect measured data from PMUs and PQM for DER/load models parameters' identification as well as model validation. So far, data for voltage and frequency disturbances for the following sites have been analysed, as shown in Table 1. Note that in all these feeders the DERs penetration is high.

Table 1: Location of PMUs and high-speed PQMs.

Measurement point (Device)	Voltage level	Customer Type	Owner
Kingston, TAS (PMU)	11 kV	Residential, Commercial	TasNetworks
Currimundi, QLD (PQM)	11 kV	Predominately Residential	Energy Queensland
Palmwoods central, QLD (PQM)	33 kV	Predominately Residential	Energy Queensland
Brendale 14B, QLD (PQM)	11 kV	Commercial	Energy Queensland
Parkhurst_Norman, QLD (PQM)	11 kV	-	Energy Queensland

Energy QLD supplied data from high-speed PQMs at above locations in their network, on disturbances occurring between December 2016 and January 2018. The measurement was triggered on disturbances exceeding $\pm 10\%$ voltage or ± 0.5 Hz frequency. Energy QLD data are mostly related to voltage disturbances; whereas, TasNetworks data are related to frequency disturbances. In the following the performance of DERs for voltage and frequency disturbances are analysed in more detail.

3.1 Voltage Disturbances

To understand the performance of DERs, it is important to review the AS4777.2-2015 requirements and then analyse their performance in the context of the AS4777.2-2015.

3.1.1 Australian standards

Australian Standard AS4777.2-2015 includes a definition of required behaviour of distributed inverters during disturbances, as listed in Table 2. Network businesses typically require compliance with this standard as a condition of connection. The Clean Energy Council (CEC) maintains a list of inverters that have been tested to be compliant with the standard.

AS4777.2-2015 requires that *"for sustained variation of the voltage and frequency beyond each limit specified the automatic disconnection device shall operate no sooner than the required trip delay time, and before the maximum*

disconnection time. This requires the inverter to remain in continuous, uninterrupted operation for voltage variations with a shorter duration than the trip delay time. When the voltage falls below the under-voltage limit it is permissible to continue, reduce or stop the inverter output during the trip time delay and if voltage returns above the limit during the trip time delay period it may resume normal operation" [3].

Table 2: Voltage set-point values defined in AS4777.2-2015.

Protective function	Protective function limit	Trip delay time	Maximum disconnection time
Undervoltage ($V <$)	180 V (0.78 pu)	1 s	2 s
Overvoltage 1 ($V >$)	260 V (1.13 pu)	1 s	2 s
Overvoltage 2 ($V >>$)	265 V (1.15 pu)	-	0.2 s

Rooftop-PV systems installed prior to October 2016 are anticipated to demonstrated behaviour aligned with the AS4777.3-2005, which requires: "If the voltage goes outside the range V_{min} to V_{max} , the disconnection device shall operate within 2 s [4]." V_{min} and V_{max} are defined as permissible ranges, listed in Table 3. Limits for sustained operation are not defined.

Table 3: Voltage set-point values defined in AS4777.3-2005.

Protective function	Single phase systems	Three phase systems	Maximum disconnection time
V_{min}	200 – 230 V (0.87 – 1.00 pu)	350 – 400 V (0.87 – 1.00 pu)	2 s
V_{max}	230 – 270 V (1.00 – 1.17 pu)	400 – 470 V (1.00 – 1.17 pu)	2 s

3.1.2 Energy Queensland data - Currimundi feeder

One of the monitors was placed at the 11 kV Currimundi feeder in South East Queensland. This feeder supplies predominantly residential load and features one of the highest penetration levels of rooftop PV in QLD. Data from several events recorded at this location, while DERs were in service, are summarised in Table 4 below. In the following event 1 is discussed in more detail.

3.1.2.1 Event 1 – 15th February 2017, 10:34 am

This event occurred at 10:34 am on 15th February 2017. AEMO's forecasting data from that five-minute period suggests that nearby rooftop PV systems were operating at approximately a 70% capacity factor at that time. Data recorded during the event is shown in Figure 13.

The initiating disturbance is believed to be a transmission level fault, given to the ~100 ms clearance time (consistent with transmission protection). The meter at Currimundi recorded an asymmetrical 0.84 pu fault (Phase C to ground). Following the fault, the power supply to the feeder was observed to increase by 120 kW. The most plausible explanation for this behaviour is that the disturbance caused a proportion of distributed PV systems

downstream of the meter to disconnect, reducing their supply to the grid. This caused the net load to increase following the event.

Table 4: Currimundi feeder voltage disturbance events summary.

Event	Affected phase	Voltage dip, distribution system	Voltage dip, inverters' terminals	Net demand increase	PV capacity factor	Equivalent full-size inverter trip
1	C	0.84 pu	0.80 pu	120 kW	70 %	172 kW
2	B	0.89 pu	0.85 pu	90 kW	70 %	129 kW
3	B	0.82 pu	0.78 pu	110 kW	25 %	440 kW

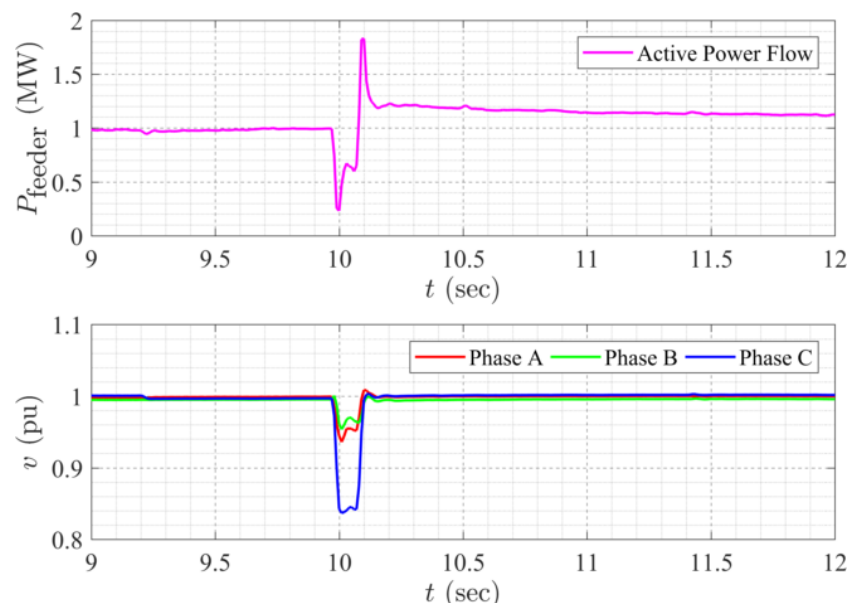


Figure 13: Event 1 – 0.84 pu asymmetrical fault measured at Currimundi (Wednesday 15th February 2017, 10:34 am), active power and voltage.

Note that in distribution systems voltage usually drops along the feeder depending on the feeder characteristic, load, voltage control strategy, and penetration of DERs. However, when the power flows from the substation to the load, it is anticipated that the voltage along the feeder drops. In general, this can be 3 % to 5 %. In this report, we assume an average of 4 % (0.04 pu) voltage drop from the substation to inverter terminals. Considering this, a 0.84 pu voltage dip at the substation corresponds to a distribution level voltage during the fault of around 0.80 pu (184 V). Inverters installed post Oct 2016 should remain in operation for voltage dips as low as 180V. Inverters installed prior to this date are specified to have voltage trip settings in the range 200-230V, which may have tripped during this event.

Figure 14 shows instantaneous values of voltage and current for Phase C (the faulted phase) at the time of the disturbance. A phase angle change between the voltage and current of around 70° is observed (highlighted in the

pink dashed circle). Bench testing suggests that many distributed PV inverters may disconnect when exposed to a voltage phase angle change, likely due to maloperation of protection or PLL measurement errors. However, there is no evidence to support that a power factor angle change also causes inverters to trip. Hence, this will be investigated further. To investigate the voltage angle change, in this case, an ideal sine wave based on the initial angle and amplitude of the measured values was generated and both the measured values and the ideal sine waves were plotted on the same figure to investigate the voltage angle change as illustrated in Figure 15. As shown, the voltage angle change is insignificant (5°) and very unlikely to be the reason for DER disconnection.

It appears plausible that some inverters, which were installed prior to Oct 2016, may have tripped due to voltage trip settings.

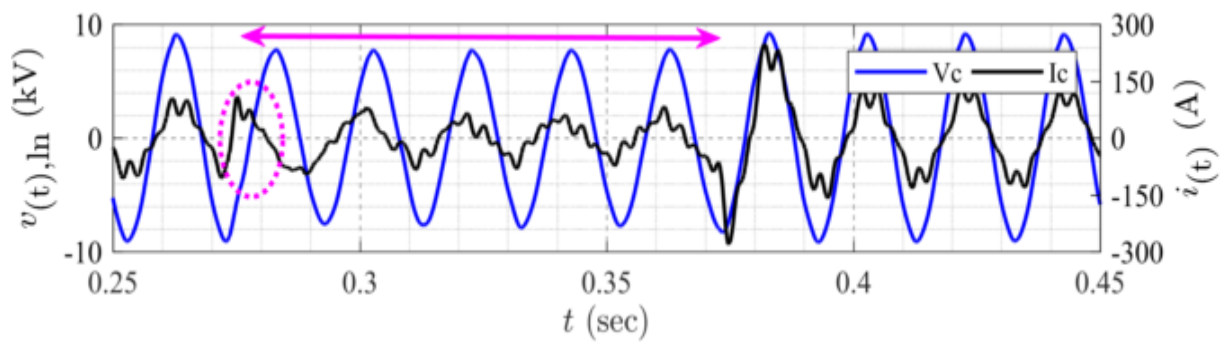


Figure 14: Event 1 – 0.84 pu asymmetrical fault measured at Currimundi (15th February 2017, 10:34 am), instantaneous voltage and current for phase C.

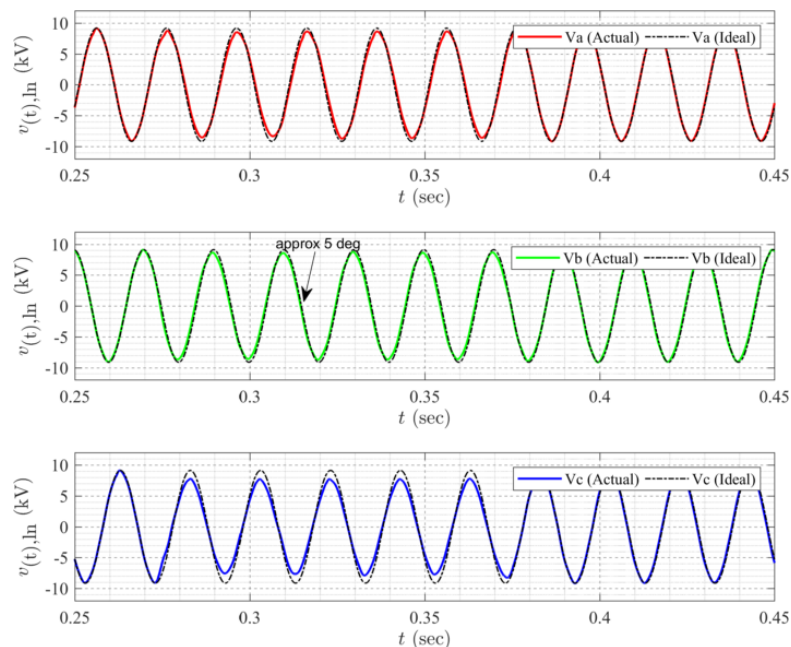


Figure 15: Event 1 – 0.84 pu asymmetrical fault measured at Currimundi (15th February 2017, 10:34 am), the instantaneous voltage for all phases.

Note that most of the rooftop-PV in the residential areas are single phase. Hence, it is difficult to compare the results of asymmetrical faults that have affected different phases and make conclusions because the number of inverters in each phase might be different. To do this, more data set are required.

3.1.3 Summary

The investigation of the events for this Energy Queensland feeders listed in Table 1 indicates that even for transmission level faults there is a possibility of rooftop-PV inverters tripping. It has been noticed that for asymmetrical faults (i.e., single-phase to ground, phase to phase or phase to phase to ground), the proportion of PV inverter cessation was higher compared to symmetrical faults. To identify the root cause of this issue, further investigation is required. This will be done by adding more tests on inverter bench testing, analysing more historical events as well as modelling and simulation.

Notice that these events were localised, with the fault and associated voltage changes only affecting a section of the network. Localised events are not of concern for bulk power system security, because only a small proportion of distributed PV systems are affected. However, larger faults may affect much larger geographical areas, as was observed in the 3rd March 2017 event in South Australia, where faults caused disconnection of distributed PV systems across the entire region. Faults also affect larger geographical areas as system strength declines over time. This means that the PV disconnection responses observed in these localised events highlight an emerging risk that will escalate as PV penetration levels increases.

3.2 Frequency Disturbances

3.2.1 Australian standards

Australian Standard AS/NZ4777.2-2015 includes a definition of required behaviour of distributed inverters during frequency disturbances:

- For a sustained variation of the voltage and frequency beyond each limit specified the automatic disconnection device shall operate no sooner than the required trip delay time, and before the maximum disconnection time (see Table 5).
- The inverter shall be capable of supplying rated power between 47 Hz and 50.25Hz.
- When a grid disturbance results in an increase in grid frequency which exceeds 50.25Hz, the inverter shall reduce the power output linearly with an increase of frequency until 52Hz is reached [3], please check Figure 7.
- The output power shall remain at or below the lowest power level reached in response to an over-frequency event between 50.25 Hz and 52 Hz. This is to provide hysteresis in the control of the inverter. When the grid frequency has decreased back to 50.15 Hz or less for at least 60s, the power level shall be increased at a rate no greater than the power rate limit (16.67% of rated power per minute). No delay in response to a frequency change is required, although it is acceptable to have a delay due to an inherent inverter system control mechanism.

Table 5: Frequency set-point values defined in AS4777.2-2015.

Protective function	Protective function limit	Trip delay time	Maximum disconnection time
Under-frequency ($F <$)	47 Hz	1 s	2 s
Over-frequency ($F >$)	52 Hz	-	0.2 s

The previous standard, AS4777.3-2005 applied prior to 9th October 2016. That standard requires: “*If frequency goes outside the range f_{min} to f_{max} , the disconnection device shall operate within 2s.* [4]” f_{min} and f_{max} are defined as permissible ranges, listed in Table 6. Limits for sustained operation are not defined.

Table 6: Frequency set-point values defined in AS4777.3-2005.

Protective function	Protective function limit	Maximum disconnection time
f_{min}	45 - 50 Hz	2 s
f_{max}	50 -55 Hz	2 s

These standards provide an important context for understanding the observed behaviour of DER during power system disturbances, as presented in the following sections.

3.2.2 Frequency trip settings

3.2.2.1 Germany’s “50.2Hz problem”

In 2005–06, Germany introduced a requirement that all generating plants connected to the low voltage network, including PV, must switch off immediately if power system frequency increased to 50.2 Hz.

In 2006, a power system event occurred at 2200 hrs that saw the frequency exceed 50.2 Hz. Subsequent analysis showed that if the event had occurred during a period of solar generation, a simultaneous shutdown of all of the nation’s PV systems could have occurred, causing further grid disruption.

This compromise to power system security prompted the German government to mandate new frequency settings for both new and existing PV installations, requiring hundreds of thousands of installations to be retrofitted. Over 315,000 PV inverters connecting PV systems larger than 10 kW were retrofitted, at a cost of approximately €175 million (\$250 million AUD) [5].

This has become a well-known example of the importance of ride-through requirements and considering bulk system security when determining performance standards for distributed resources.

3.2.2.2 Survey of frequency trip settings in the NEM

In response to the German experience, in 2015 AEMO conducted a study to ascertain whether the inverters that currently connect small-scale PV generation to Australian networks may also respond simultaneously to frequency disturbances by disconnecting at a set frequency [6].

AEMO obtained frequency trip setting data for 44 % of the total installed capacity of inverters as at May 2015, and analysis of this data showed there is a spread in the frequency settings and timing of when inverters will trip. This indicates a low probability of inverters tripping in unison due to frequency disturbances within the required frequency operating ranges.

The frequency trip settings information collected is summarised in Table 7 and Table 8. This survey provides a valuable foundation for interpreting legacy PV system behaviour observed during power system disturbances, and the development of accurate dynamic models, as outlined in the following sections.

Table 7: Frequency trip settings of distributed PV for under-frequency events (as of May 2015).

Settings		Distribution of frequency settings across available data			
Frequency (Hz)	Pickup time (seconds)	NEM	South Australia	Queensland	Tasmania
49.02	1.9	0.2%	0.2%	0.2%	0.1%
49.01	0.18	2.8%	1.9%	1.8%	0.8%
49	0.06	14.1%	12.4%	14.7%	17.6%
49	1.96	0.7%	0.2%	0.2%	1.0%
49	2	0.1%	0.1%	0.0%	0.0%
48.52	2	1.0%	1.0%	2.3%	0.0%
47.6	1.8	2.3%	2.2%	0.1%	6.5%
47.55	0.2	3.4%	4.9%	7.0%	2.0%
47.5	1.8	5.7%	3.2%	7.3%	5.8%
47.1	1.8	15.6%	9.0%	24.2%	22.2%
47	1.6	0.5%	0.0%	0.0%	0.0%
<47	-	53.5%	65.0%	42.3%	43.4%

Table 8: Frequency trip settings of distributed PV for over-frequency events (as of May 2015).

Settings		Distribution of frequency settings across available data			
Frequency (Hz)	Pickup time (seconds)	NEM	South Australia	Queensland	Tasmania
50.98	1.9	0.2%	0.2%	0.2%	0.1%
50.99	0.18	2.8%	1.9%	1.8%	0.8%
51	0.06	14.1%	12.4%	14.7%	17.6%
51	1.96	0.7%	0.2%	0.2%	1.0%
51	2	0.1%	0.1%	0.0%	0.0%
51.58	2	1.0%	1.0%	2.3%	0.7%
51.9	1.8	2.3%	2.2%	0.1%	6.5%
52	1.6	0.5%	0.0%	0.0%	0.0%
52	1.8	5.7%	3.2%	7.3%	5.8%
>52	-	72.5%	78.9%	73.4%	67.6%

3.2.3 TasNetworks data – Kingston feeder

Tasmania has relatively lower levels of distributed PV installed compared with some other NEM regions. However, it provides a valuable case study for understanding DER behaviour during disturbances, because as a relatively smaller island power system, Tasmania often experiences frequency disturbances that provide insight into aggregate DER behaviour during those events.

TasNetworks has installed a phasor measurement unit (PMU) at the 11 kV Kingston feeder. This feeder has a relatively high level of distributed PV installed, with approximately 1.0 MW of distributed PV capacity on the monitored feeder².

Five events of interest have been analysed, with preliminary findings summarised in the following table.

² The total installed PV in Kingston area with postcode 7050 is around 3 MW distributed among three feeders. It is assumed that the PV installation is uniformly distributed among these three feeders.

Table 9: Kingston feeder frequency disturbance summary

Event	Date	Time	Frequency Nadir	PV performance	$\Delta P_{\text{feeder}}^3$	AUFLS2 ⁴ in service	DER Trip
1	13 Aug 2018	08:43:14	48.73 Hz	21 % (0.21 MW)	0.15 MW	Yes	Unlikely
2	25 Aug 2018	13:11:41	48.72 Hz	44 % (0.44 MW)	0.24 MW	Yes	Likely
3	06 Sep 2018	12:43:58	48.57 Hz	17 % (0.17 MW)	0 MW	No	No
4	10 Sep 2018	08:24:47	48.56 Hz	18 % (0.18 MW)	0.06 MW	No	No
5	06 Sep 2018	02:01:57	48.79 Hz	N/A	0.13 MW	Yes	N/A

From the above, possible DER trips have been observed in Event 2, where the DER operates with 44 % capacity factor. Hence, this event is analysed in more detail in the following.

3.2.3.1 Event 2 – 25th August 2018, 1:11 pm

This event occurred at 1:11 pm on 25th August 2018, associated with a mainland event (separation of Queensland and South Australia). It is estimated that distributed PV was operating at a capacity factor of around 44 % at the time of the event or generating around 0.44 MW on this feeder. The feeder was supplying a net load of approximately 3.5 MW. Tasmanian frequency, and the active power supplied to the Kingston feeder are illustrated in the Figures below.

³ $P_{\text{feeder_post_event}} - P_{\text{feeder_pre_event}}$.

⁴ AUSFL2 is an under-frequency control scheme, which switches off a specific amount of load. Current pick-up frequency is set to 48.8 Hz.

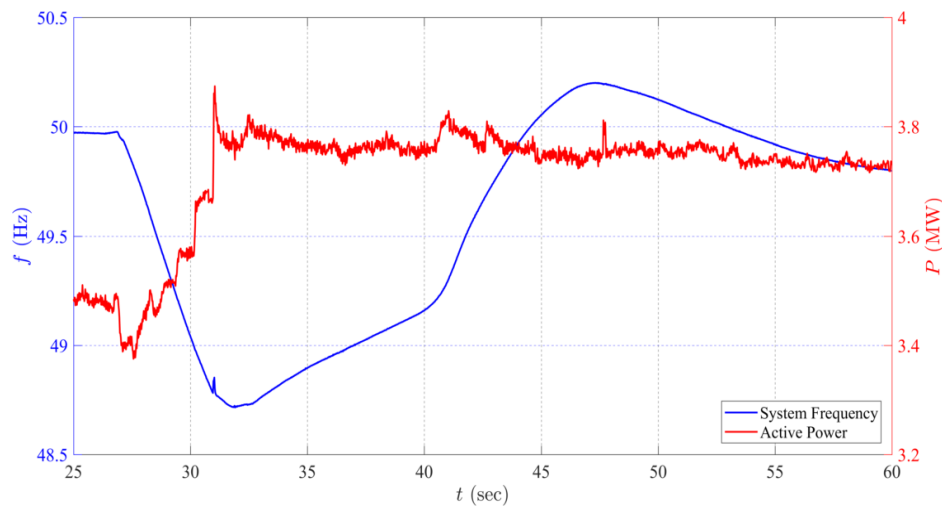


Figure 16: Event II – 25 August 2018, 1:11 pm

In this event, the frequency is observed to fall from 49.95 Hz to 48.72 Hz over a period of around five seconds. The active power supplied to the Kingston feeder is observed to increase in steps from 3.5 MW to 3.74 MW.

The Figure below shows an expanded version of the event. The point at which frequency reaches 49 Hz is indicated. The largest increase in active power (~140 kW) occurs around 0.86 seconds (860 ms) after the frequency reaches 49 Hz, or 250 ms after the frequency reaches 48.8 Hz, this behaviour was observed in Event 1 as well. The earlier increase in active power (~100 kW) occurs around 80 ms after the frequency drops below 49 Hz. The latter is consistent with the AEMO survey results shown in Table 7. A 100 kW increase 80 ms after frequency reaches 49 Hz represents trip of around 20 % inverters. The 140 kW increase might be due to a combination of voltage increase as well as inverters trips, as shown in Figure 17.

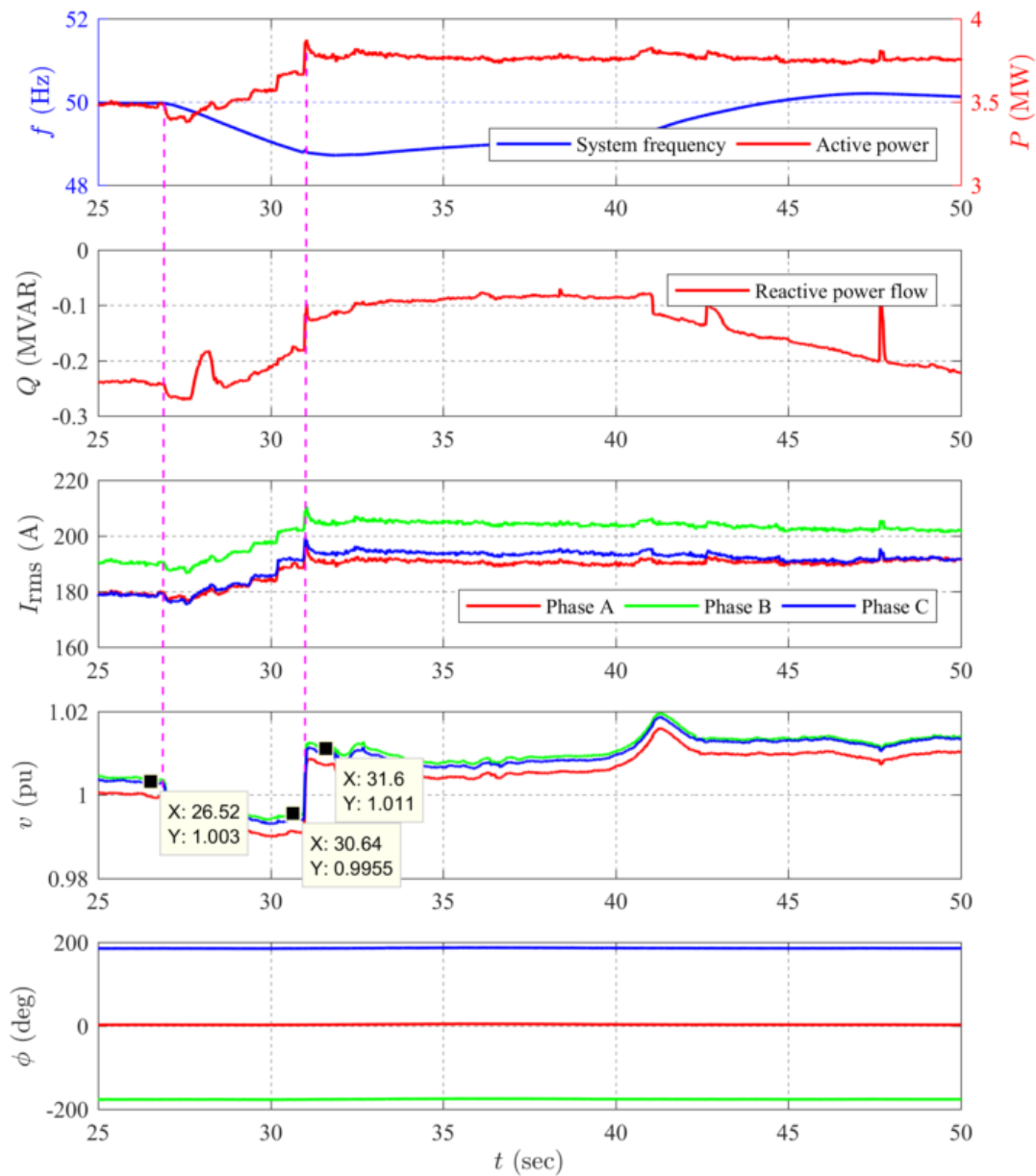


Figure 17: Event II – 25 August 2018, 1:11 pm, all channels

Figure 17 shows that when the frequency reaches 49 Hz, the voltage is relatively constant. This again confirms the earlier claim that 100 kW increase at this point might be due to inverters tripping. Whereas, when the frequency reaches 48.8 Hz and the AUFLS2 operates and disconnect some of the loads in Tasmania, there is a sudden increase in voltage, which in turn results in a sudden increase in active and reactive power of the feeder due to voltage dependency of the load, as highlighted with pink lines on the figure.

This event demonstrates the importance of composite load modelling. To quantify the contribution of the load's voltage/frequency dependency on active power, an accurate representation of load dynamic is essential.

3.2.3.2 Summary

To estimate an approximate value for voltage dependency of the load in this feeder, we consider Event 5. In this event, for 4.25 % voltage increase the active power increases by 0.13 MW, when the feeder load was 3.44 MW, which corresponds to 0.0378MW/MW increase. Considering this, the voltage dependency of the load would be $((0.00872\text{MW/MW})/(1\%\Delta v))^5$. Applying this to Event II, where the voltage increase is 2% and the active power flow is 3.5 MW, gives us $((0.00872\text{MW/MW})/(1\%\Delta v)*2\%*3.5\text{MW}) = 0.0622\text{MW}$. Let the uncertainty due to load composition to be around 40%, so the active power flow increase should have been 100 kW at 48.8 Hz. As noticed, the increase in the active power flow of the feeder was 140 kW. This clearly indicates that this could have been due to both the voltage dependency of the load as well as DER trip. Further investigation is required to quantify the contribution of each.

⁵ Note that load can have very nonlinear behavior and should be modeled explicitly. This coefficient should not be used for other purpose. It is just an indicative number. Also, load composition might vary with time (e.g., 3 MW at night time might represent different load composition compared to 3 MW load during the day).

4 DER model development

The bench testing results and measured data discussed in the previous chapters highlight that DER behaviour during disturbances has a significant impact on power system performance. This means it is becoming increasingly important that DER is represented accurately in AEMO's dynamic models so that it can be properly accounted for in stability studies. Furthermore, in developing and verifying suitable models for DER, it is important to update the representation of the load in dynamic models, since the two are intimately connected.

Representing many millions of diverse customer devices in a dynamic model is inherently challenging. The model must capture the diverse behaviour of aggregated DER during a wide range of disturbances, considering the many different makes and models of systems installed, the many different settings applied to those systems, and the different properties of the network locations where they are installed. As highlighted throughout the previous chapters, DER behaviour is complex and multifaceted, and there is limited information available upon which to base model assumptions.

Load behaviour could be considered even more complex and difficult to capture. Historically, residential loads consisted primarily of resistive heating, cooking, and incandescent lighting, along with small induction motors driving small appliances and some residential air conditioners. Today, loads are transitioning to more advanced and higher efficiency options, many including power electronic converters based. It is also important to capture the breadth of load types, including not just residential, but also industrial and commercial loads, all of which form large and important components.

Furthermore, the composition of load changes considerably on an hourly, daily and seasonal basis. This means load models must be adaptable by the time of day and season, supported by accurate information on load composition at different times and locations.

The challenge is to develop an aggregate model of load and DER behaviour that is accurate, but also simple enough to be useful for daily power system studies.

There is very little information available about the composition of electrical load in Australia, and even less information about how those many different types of loads behave during power system disturbances. A considerable work program is required to develop the necessary information.

4.1 International work

The development of dynamic load models has been a topic of international analysis and research for multiple decades. There has been a significant body of work pursued in the Western Interconnection in the USA (led by the Western Electricity Coordinating Council, WECC) over the past few decades, culminating in the specification of a dynamic "composite load model [7]" in 2015. The model includes a simplified aggregate representation of the distribution network, an aggregate representation of DER ("Distributed Generation", or DG), and six types of customer loads [8], as also shown in Figure 18:

- Motor A - Three-phase induction motors with low inertia, driving constant torque loads. Typically includes commercial/industrial air conditioning compressors and refrigeration systems in the USA.
- Motor B – Three-phase induction motors with high inertia, driving loads whose torque is proportional to speed squared. Typically includes motors found in commercial ventilation fans and air-handling systems.
- Motor C – Three-phase induction motors with low inertia driving loads whose torque is proportional to speed squared. Typically includes motors found in commercial water circulation pumps in central cooling systems.
- Motor D – Single-phase induction motors representing primarily residential air conditioner compressor motors. In Australia, air conditioning loads might be connected to the grid via power electronic converters, this will be investigated.
- Electronic load – Power electronic loads (inverter-based or electronically coupled).
- Static load – Other types of loads not explicitly modelled in the other components. Includes lighting, small electrical household and small commercial loads.

The structure of the model including DG is illustrated in the Figure below.

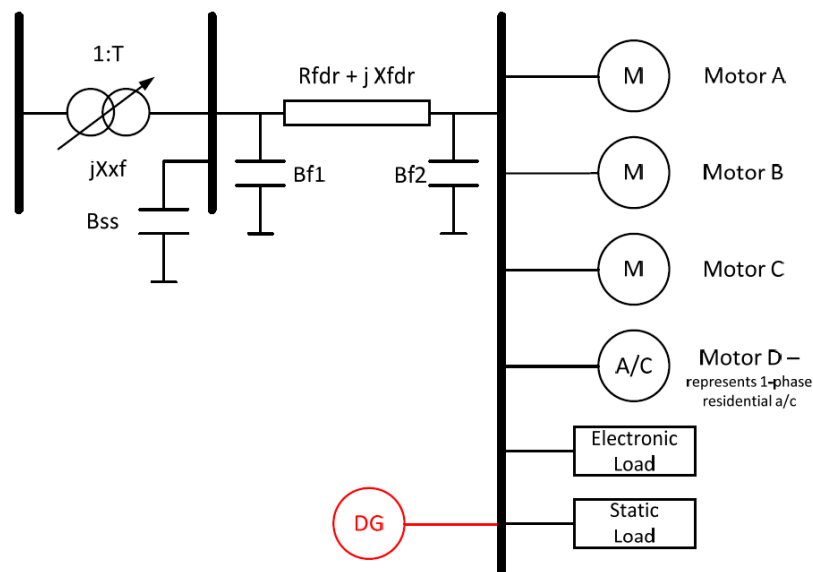


Figure 18: Composite Load Model with Distributed Generation (DG).

System operators can apply this model to the individual features of their own power system by specifying the proportions of DER and each load type (as a function of location and time period), and by specifying the parameters of each component of the model to represent the trip settings, dead-bands, response times and other individual behaviours of those loads in that power system. NERC has provided guidance to system operators in the USA on how to proceed with collecting the necessary data and developing the necessary parameters [8], [9]. This provides a useful starting reference for AEMO in embarking on a similar body of work.

The DER model has been a recent focus of attention in the WECC working groups. A final version was published in September 2018 [1], and working groups are establishing default parameters at present. The model includes the capabilities of representing frequency responsive behaviour, Volt-watt functions, frequency tripping behaviour, and an aggregate representation of voltage tripping behaviour, intended to emulate the gradient of voltage along a feeder. All aspects are represented for the DER fleet in aggregate, at a specific transmission connection point, and a specific point in time. This model will be used as a starting point, as shown in Figure below.

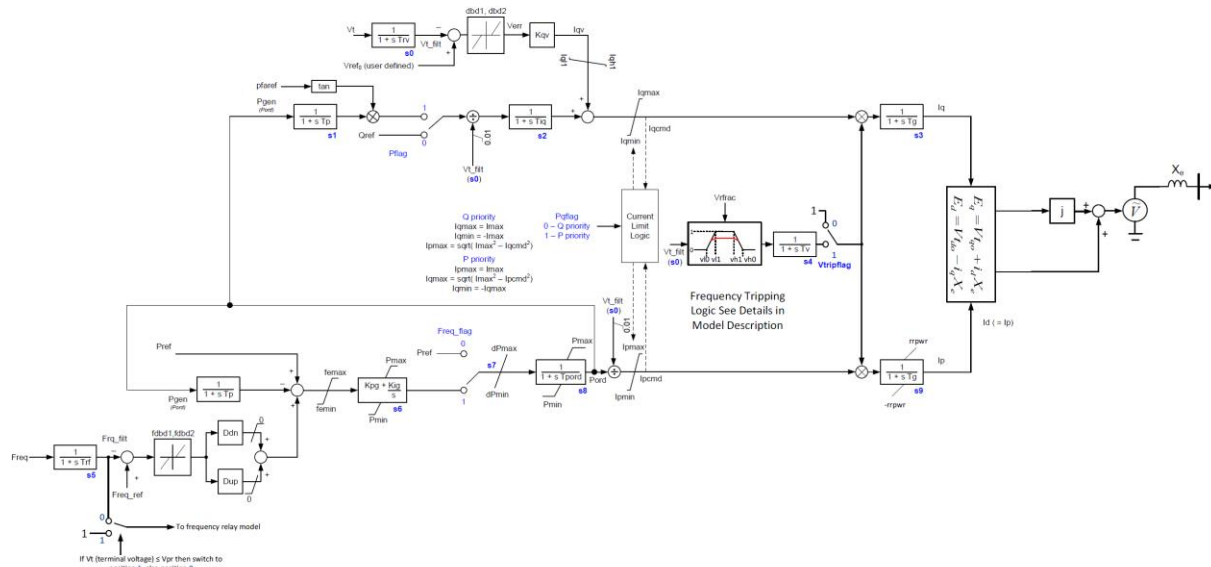


Figure 19: proposed DER_A model [1].

As discussed in previous chapters, frequency and voltage ride through capability in the AS4777.3-2005 and AS4777.2-2015 are defined differently. The proportion of installed PV inverters according to each standard is significant, as shown in Table 10. Hence, in this deliverable, we consider two DER models (representing 2005 and 2015 standards, as shown in Figure 20) and identify parameters for each DG model from the relevant standards.

Table 10: Proportion of PV installation according to different standards (as at Sept 2018).

State	Proportion of PV installed per AS4777.3-2005	Proportion of PV installed per AS4777.2-2015
NSW	71%	29%
QLD	76%	24%
SA	78%	22%
VIC	74%	26%
TAS	75%	25%

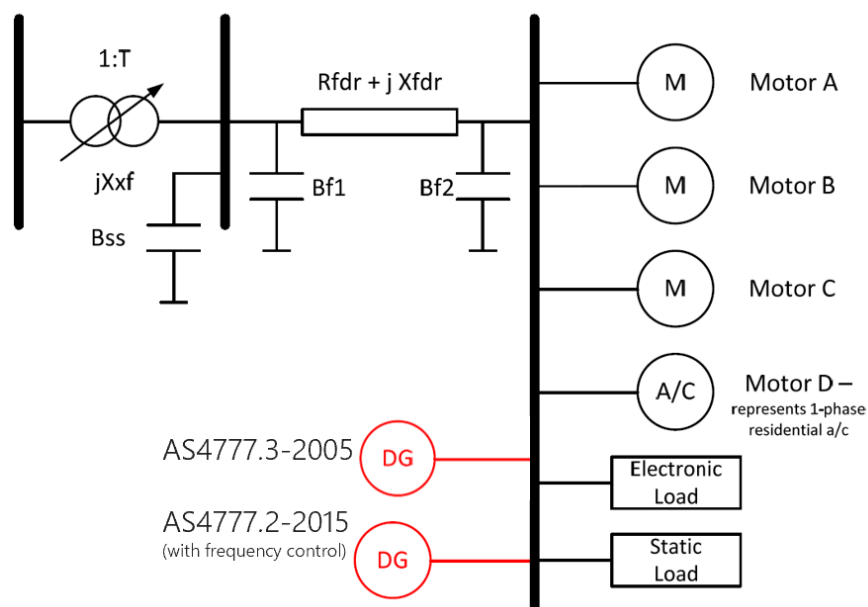


Figure 20: Proposed composite load and DER model, based on the WECC model.

4.2 DER parameters per AS4777

As shown in previous chapters, the settings of inverters do not necessarily according to the specified standard, e.g., Table 7 and Table 8 show that the frequency trip settings of inverters are significantly different from those specified in AS4777.3-2005. At this stage, there is not enough data from the monitored feeder to make a general conclusion on the aggregated parameters for voltage and frequency trip settings. Hence, settings and parameters for the DER model will be based on AS4777.3-2005 and AS4777.2-2015, as shown in the following Table. It has to be mentioned that the voltage and frequency trip settings in those two standards are significantly different. Therefore, two distinct models are proposed at this stage as shown in Figure 20. Note that it is possible to have a single aggregated DER model for all inverters (i.e., those based on AS4777.3-2005 and AS4777.2-2015) and identify their aggregated voltage trip by further tuning parameters J+22 to J+30 (column 2 of Table 11) of the model. However, integration of frequency trip setting in single model required augmentation of the base model, which is possible but requires lots of efforts.

Table 11: DER parameters per AS4777

Aspect	PSSE ref ⁶	Parameter	Unit	AS4777.2-2015 Settings	AS4777.3-2005 Settings	Description
Reactive power	M	PfFlag	-	1	1	1: Constant power factor mode

⁶ M refers to ICON, settings and J refers to CONs, constants or parameters.

Frequency control	M+1	FreqFlag	-	1	0	0: disabled
Current control	M+2	PQFlag	-	1	1	1: Priority for current limit
Type of unit	M+3	GenFlag	-	1	1	1: unit is a generator ⁷
Voltage trip	M+4	VtripFlag	-	1	1	1: enabled
Frequency trip	M+5	FtripFlag	-	1	1	1: enabled
Voltage Control	J	T _v	sec	0.02	0.02	Voltage measurement transducer time constant
Frequency Control	J+1	T _f	"	0.02	0.02	Frequency measurement transducer time constant
Voltage Control	J+2	dbd1	pu	-0.02	-0.02	Lower voltage dead-band (<= 0)
"	J+3	dbd2	"	0.02	0.02	Upper voltage dead-band (> 0)
"	J+4	K _{qv}	"	0	0	Proportional voltage control gain
"	J+5	Vref0	"	1	1	user specified voltage set-point
Voltage and frequency	J+6	T _p	sec	0	0	Power measurement transducer time constant
Voltage Control	J+7	T _{iq}	"	0.02	0.02	Q-control time constant
Frequency control	J+8	D _{dn}	pu	28.57 ⁸	0	Reciprocal of droop for over-frequency conditions
"	J+9	D _{up}	"	0	0	Reciprocal of droop for under-frequency conditions (> 0)
"	J+10	fdbd1	"	-0.005	0	Dead-band for frequency control, lower threshold (<= 0)

⁷ For battery inverters, this is 0.

⁸ Based on $((52-50.25)/50) = 3.5\%$ droop.

“	J+11	fdbd2	“	0	0	Dead-band for frequency control, upper threshold (≥ 0)
“	J+12	femax	“	99	99	Frequency error upper limit
“	J+13	femin	“	-99	-99	Frequency error lower limit
“	J+14	PMAX	“	1	1	Maximum power limit
“	J+15	PMIN	“	0	0	Minimum power limit
“	J+16	dPmax	pu/sec	0	99	Power reference maximum ramp rate
“	J+17	dPmin	“	-99	-99	Power reference minimum ramp rate
“	J+18	Tpord	sec	0	0	Power filter time constant
“	J+19	Kpg	pu	0	0	Active power controller proportional gain
“	J+20	Kig	“	10	10	Active power controller integral gain
P-Q priority	J+21	Imax	“	1	1	Maximum converter current
Voltage ⁹ tripping	J+22	vl0	pu	0.78	0.87	Inverter voltage break-point for low voltage cut-out
“	J+23	vl1	“	0.82	0.91	Inverter voltage break-point for low voltage cut-out ($vl1 > vl0$)
“	J+24	vh0	“	1.19	1.21	Inverter voltage break-point for high voltage cut-out
“	J+25	vh1	“	1.15	1.17	Inverter voltage break-point for high voltage cut-out ($vh1 < vh0$)
“	J+26	tvl0	sec	1.5	2	Low voltage cut-out timer corresponding to voltage vl0

⁹ An average of 4% voltage drop is considered along the feeder, this needs further analysis and will be further tuned in the future reports. This 4% represents the voltage gradient of the feeder.

“	J+27	tv1	“	1	0.1	Low voltage cut-out timer corresponding to voltage v1
“	J+28	tvh0	“	1.5	1.5	High voltage cut-out timer corresponding to voltage vh0
“	J+29	tvh1	“	2	2	High voltage cut-out timer corresponding to voltage vh1
“	J+30	Vfrac	Pu	0.5 ¹⁰	1	Fraction of device that recovers after voltage comes back to within $v1 < V < v1$ ($0 \leq Vfrac \leq 1$)
Frequency tripping	J+31	fl	Hz	47	45	Inverter frequency break-point for low-frequency cut-out
“	J+32	fh	“	52	55	Inverter frequency break-point for high-frequency cut-out
“	J+33	tfl	sec	1.5	1	Low frequency cut-out timer corresponding to frequency fl
“	J+34	tfh	“	0.1	0.1	High frequency cut-out timer corresponding to frequency fh
Current control	J+35	Tg	“	0.02	0.02	Current control time constant (to represent behaviour of inner control loops) (> 0)
Ramp rate	J+36	rrpwr	pu/sec	10	10	ramp rate for real power increase following a fault
Voltage tripping	J+37	Tv	sec	0.02	0.02	time constant on the output of the multiplier

¹⁰ At this stage, it is assumed that 50% of the DERs are disconnected when the voltage is between v10 and v11. To identify the correct proportion of the Vfrac, it is necessary to analysis further high-speed data. This will also help to better quantify v10, v11, vh0, vh1 limits.

tripping	J+38	Vpr	pu	0.7	0.7	voltage below which frequency tripping is disabled
Reactive power	J+39	Iqhl	"	1	1	Upper limit on reactive current injection Iqinj
"	J+40	Iqll	"	-1	-1	Lower limit on reactive current injection Iqinj

4.3 Time domain simulations

To evaluate the performance of DER_A model, a single machine infinite bus model (SMIB) model is developed, as shown in Figure 21. A minimum available fault level of 700 MVA was considered for grid representation. Some typical transformers and distribution lines parameters are used. For simplicity, the 400 V conductors' impedance is not considered. The DER model represents the aggregation of 1 MW rooftop-PV at 400 V level. The dynamic parameters of the model are according to Table 11, column 5 (AS4777.2-2015 Settings).

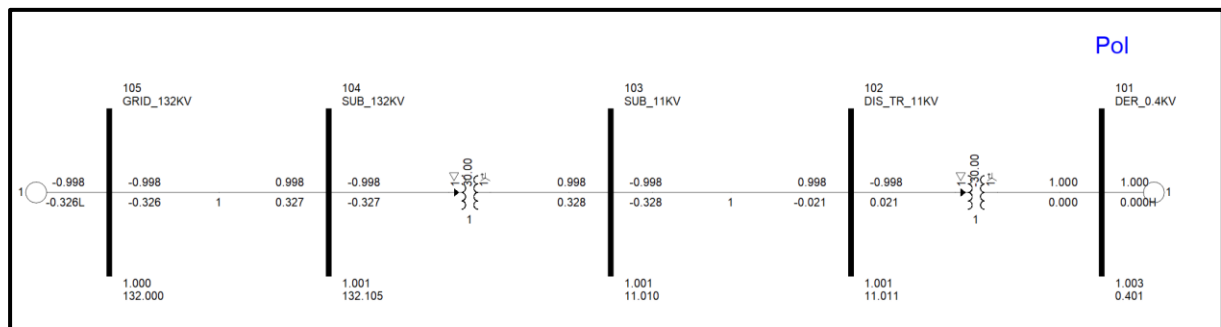


Figure 21: Single line diagram of the SMIB model in PSSE

The performance of the DER_A model is evaluated by applying some voltage and frequency disturbances.

4.3.1 Voltage disturbances

Following voltage disturbances were applied at bus 105.

4.3.1.1 V0.7 pu for 1 sec

The voltage is lower than $v_{l0}=0.78$ and it sustains for 1 sec, which is the boundary condition for $tv_{l1}=1$ sec and shorter than $tv_{l0}=1.5$ sec. Hence, it is anticipated that 100% of the inverters will remain online after the disturbance is removed. This is validated by time domain simulation results, as shown in Figure below.

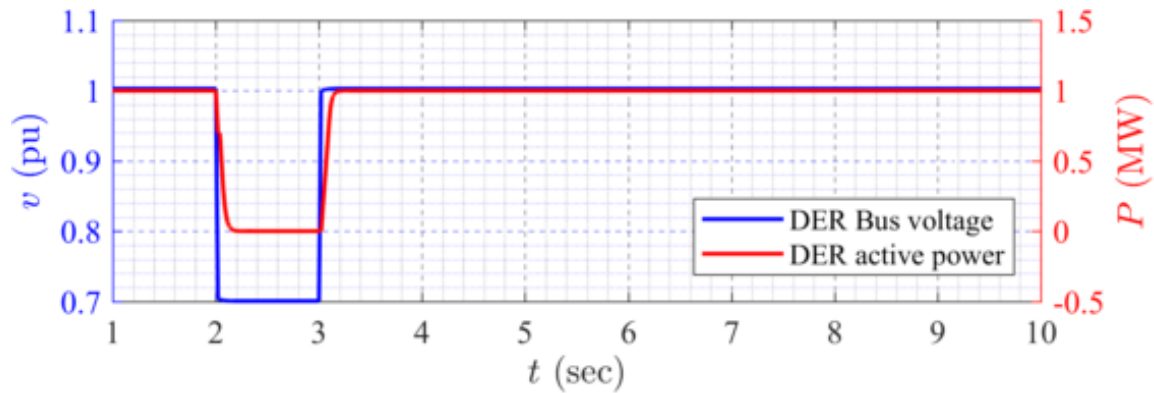


Figure 22: DER_A response to 0.7 pu voltage disturbance for 1 sec.

4.3.1.2 V 0.7 pu for 1.5 sec

The voltage is lower than $v_{l0}=0.78$ and it sustains for 1.5 sec, which is the boundary condition for $tv_{l0}=1.5$ sec and longer than $tv_{l1}=1$ sec. Since $V_{frac} = 0.5$, it is anticipated that 50% of the inverters will be disconnected after the disturbance is removed and the remaining 50% will stay online. Time domain simulation confirms this, as illustrated below.

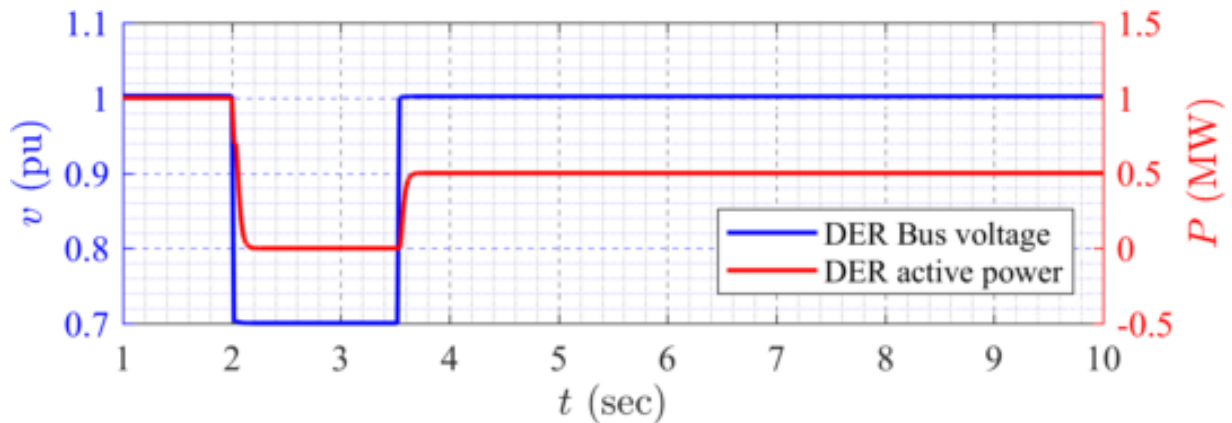


Figure 23: DER_A response to 0.7 pu voltage disturbance for 1.5 sec.

4.3.1.3 V 0.7 pu for 2 sec

Similar to the previous case the voltage is lower than v_{l0} and it remains low for 2 sec, i.e., longer than $tv_{l0}=1.5$ sec. Hence, it is expected that DER will disconnect even after the disturbance is removed, which is the case, as illustrated in the following Figure.

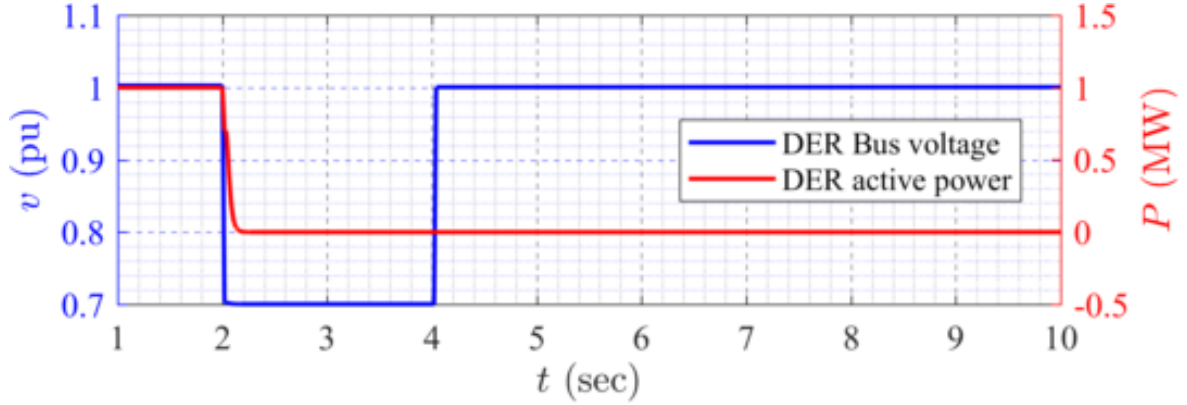


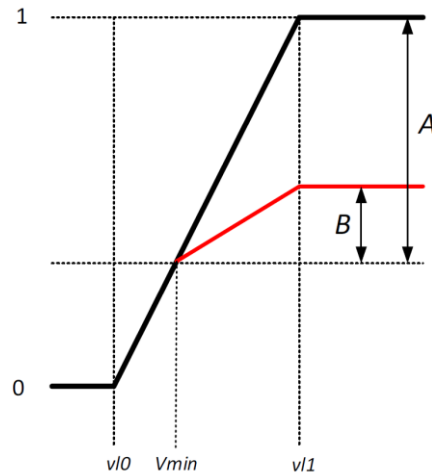
Figure 24: DER_A response to 0.7 pu voltage disturbance for 2 sec.

4.3.1.4 V 0.8 pu for 2 sec

In this case, the voltage is lower than $v_{l1}=0.82$ and higher than $v_{l0}=0.78$. It sustains for 2 sec, which is longer than $t_{vl0}=1.5$ sec. In this situation, it is anticipated that a portion the inverters, represented by a Multiplier will remain in service and the rest will be disconnected. Considering Figure 25, the Multiplier for this situation is calculated from the following formula [1]:

$$\text{Multiplier} = V_{frac} \times \left(\frac{v_{l1} - V_{min}}{v_{l1} - v_{l0}} \right) + \left(\frac{V_{min} - v_{l0}}{v_{l1} - v_{l0}} \right) \quad (1)$$

Where $V_{frac} = 0.5$, $v_{l1}=0.82$, $V_{min} = 0.8$ and $v_{l0} = 0.78$. Considering these, the Multiplier is anticipated to be ≈ 0.75 , i.e., 75% of the inverters will remain online after the disturbance is removed, which is the case, as shown in Figure 26.

Figure 25: Effect of V_{frac} on partial tripping of DER.

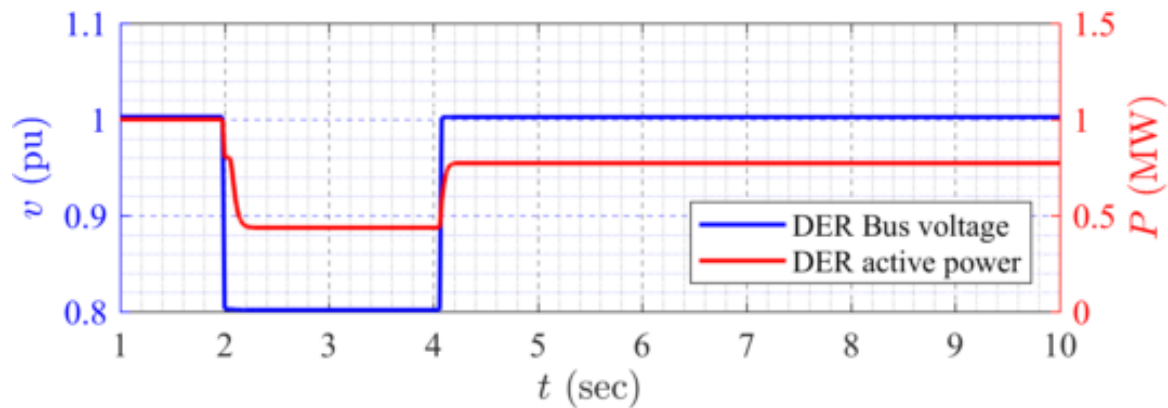


Figure 26: DER_A response to 0.8 pu voltage disturbance for 2 sec.

4.3.1.5 V 0.9 pu for 8 sec

In this case, the voltage is higher than $v_{l1}=0.82$. Hence, it is expected that no DERs should trip, as shown in Figure 25. Time domain simulation shows that all the DERs remain online; however, the active power output of the DERs reduces, proportion to its terminal voltage, as shown in Figure 27. This is correct, as the DER is modelled as a current source and its power is a linear function of voltage. The 100% utilisation of the current in Figure below confirms this.

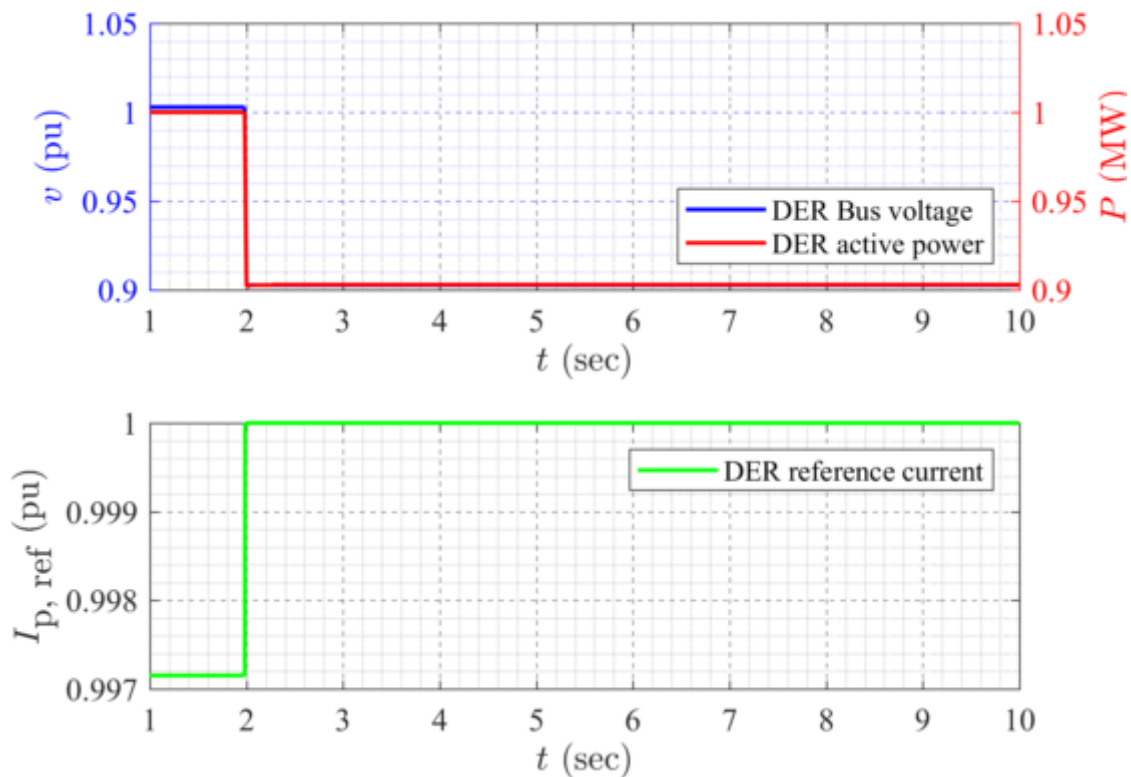


Figure 27: DER_A response to 0.9 pu voltage disturbance for 8 sec.

4.3.1.6 V 1.13 pu for 8 sec

The voltage is lower than $v_{h1}=1.15$ and it sustains for 1.5 sec. Hence, it is expected that no DERs should trip. Time domain simulation confirms this, as illustrated in Figure 28. Note that when the terminal voltage increases, DER reduces its current to achieve the 1 MW reference power.

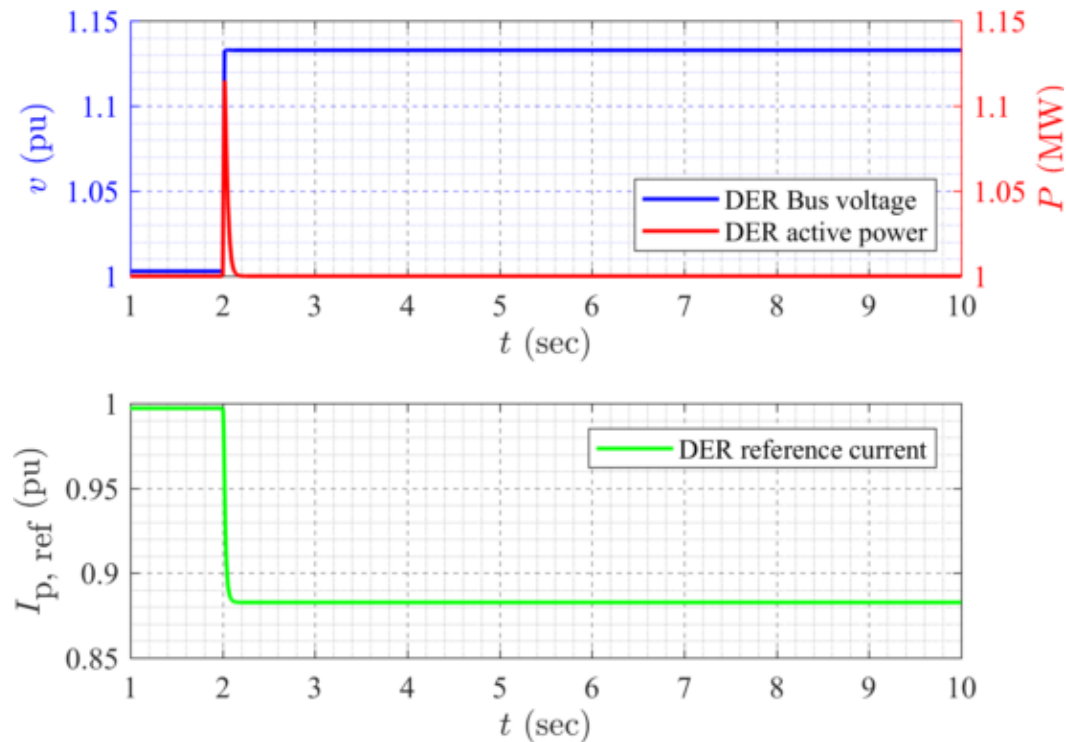


Figure 28: DER_A response to 1.13 pu voltage disturbance for 8 sec.

4.3.1.7 V 1.2 pu for 2 sec

The voltage is higher than $v_{h0}=1.19$ and it sustains for longer than $t_{vh0} = 1.5$ sec. Hence, a full DER tripping is anticipated, as shown in Figure below.

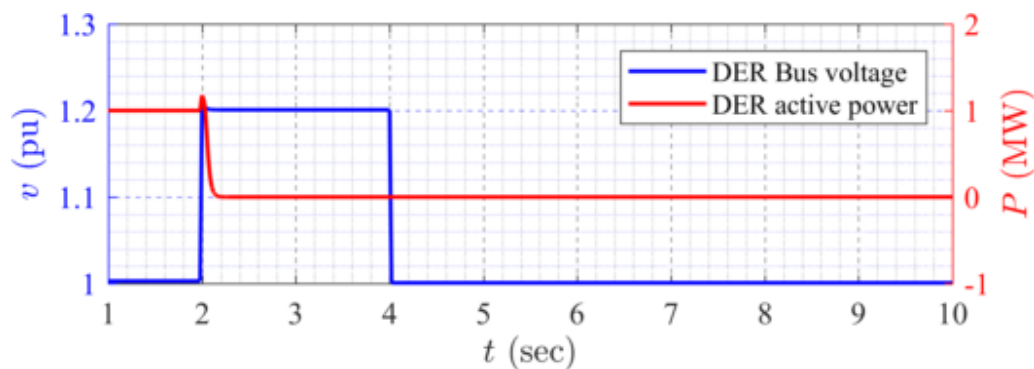


Figure 29: DER_A response to 1.2 pu voltage disturbance for 2 sec.

4.3.2 Frequency disturbances

Following frequency disturbances were applied at bus 105. It has to be mentioned that while applying frequency disturbance, a RoCoF of 4 Hz/sec is considered.

4.3.2.1 $f = 46.94$ Hz ($\Delta f = -0.0612$ pu) for 1.8 sec

The frequency is lower than $f_l = 47$ Hz for longer than $t_{fl} = 1.5$ sec. Hence, a full DER trip is anticipated after $t_{fl} = 1.5$ sec, which is the case, as shown in Figure below.

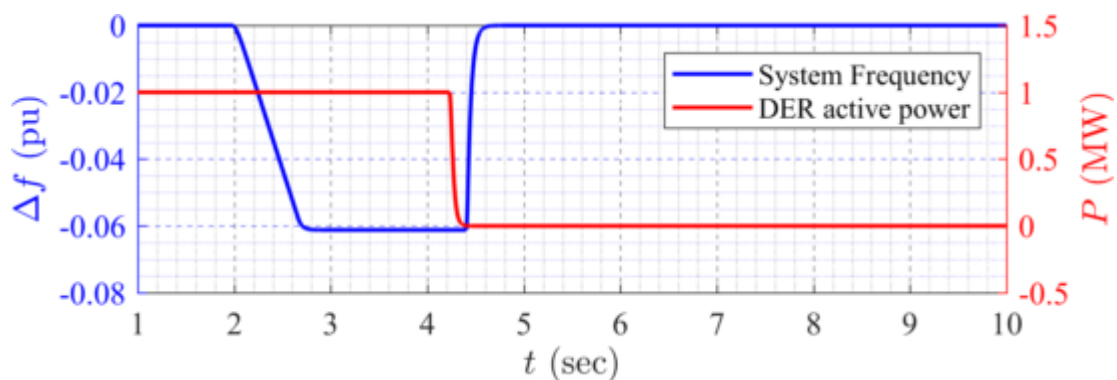


Figure 30: DER_A response to 46.94 Hz frequency disturbance for 1.8 sec.

4.3.2.2 $f = 46.94$ Hz ($\Delta f = -0.0612$ pu) for 1.4 sec

The frequency is lower than $f_l = 47$ Hz for shorter than $t_{fl} = 1.5$ sec. Hence, no DER tripping is expected, which is the case, as shown in Figure below.

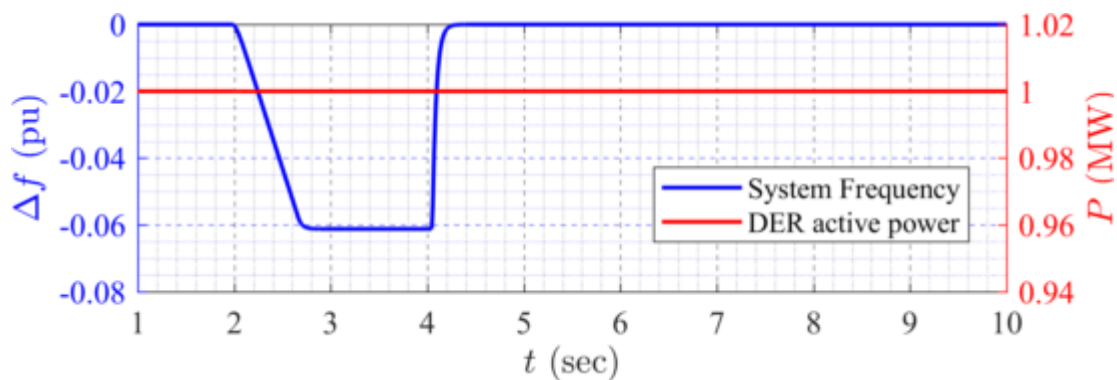


Figure 31: DER_A response to 46.94 Hz frequency disturbance for 1.4 sec.

4.3.2.3 $f = 47.02$ Hz ($\Delta f = -0.0596$ pu) for 7.25 sec

The frequency is higher than $f_l = 47$ Hz. Hence, no DER tripping is expected, which is the case, as shown in Figure below.

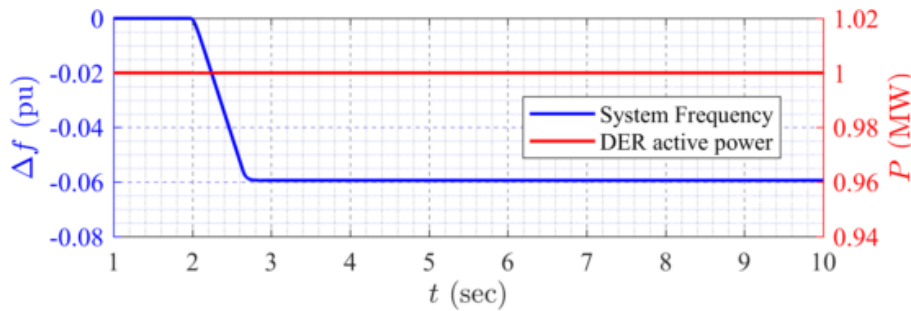


Figure 32: DER_A response to 47.02 Hz frequency disturbance for 7.25 sec.

4.3.2.4 f 51.98 Hz ($\Delta f = 0.0396$ pu) for 7.25 sec

In this case, the frequency is lower than $f_h=52$ Hz. Hence, no DER tripping is expected. Nonetheless, because of the frequency control requirement illustrated in Figure 7, it is anticipated the DER reduces its active output power, which is the case, as shown in Figure below.

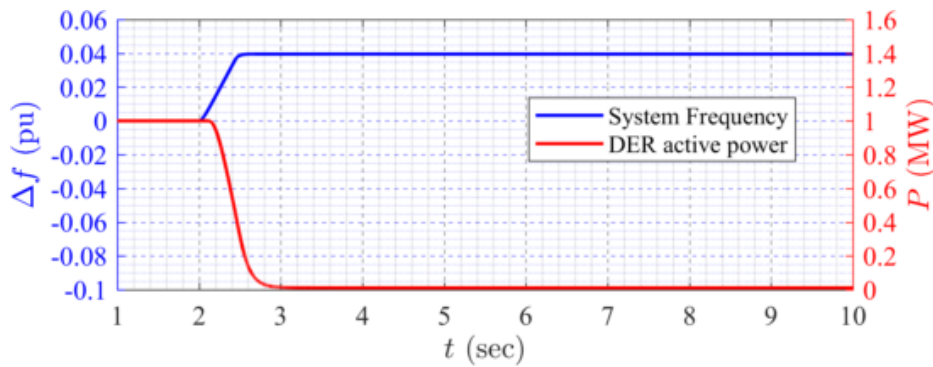


Figure 33: DER_A response to 51.98 Hz frequency disturbance for 7.25 sec.

4.3.2.5 f 52.02 Hz ($\Delta f = 0.0404$ pu) for 0.08 sec

In this case, the frequency is higher than $f_h=52$ Hz for shorter than $t_{fh} = 0.1$ sec. Hence, no DER tripping is expected. However active power reduction is expected, similar to the previous case, as shown in Figure below.

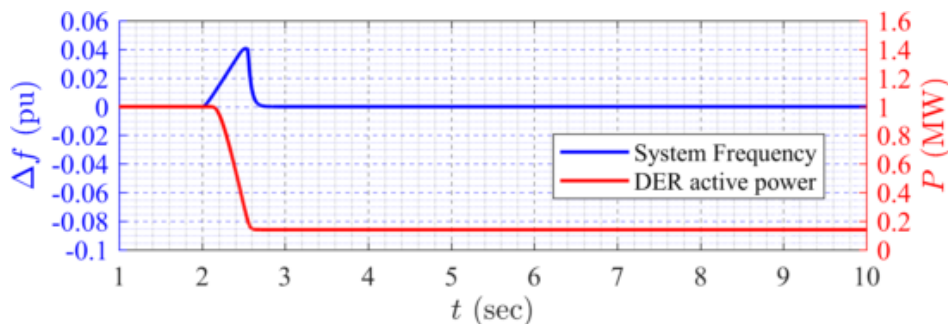


Figure 34: DER_A response to 52.02 Hz frequency disturbance for 0.08 sec.

4.3.2.6 $f = 52.02$ Hz ($\Delta f = 0.0404$ pu) for 0.2 sec

In this case, the frequency is higher than $f_h = 52$ Hz for longer than $t_{fh} = 0.1$ sec. Hence, a full DER tripping is expected 0.1 sec after the frequency reaches 52 Hz, which is the case, as shown in Figure below.

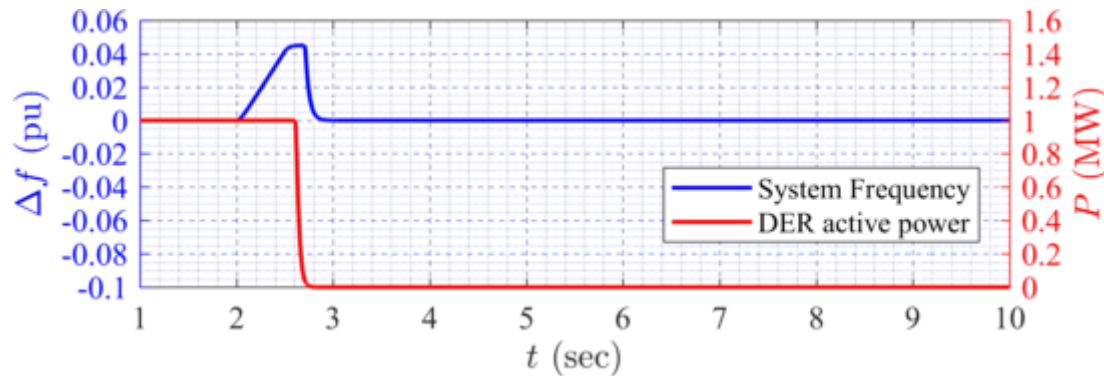


Figure 35: DER_A response to 52.02 Hz frequency disturbance for 0.2 sec.

4.4 Summary

The DER_A model is utilised to represent the aggregation of rooftop-PVs. Preliminary time domain simulation demonstrates the robustness and flexibility of the model. However, further data and analysis are required to refine the parameters related to frequency and voltage trip settings. Further, to utilise this model for BPS studies, such as NEM, it is crucial to have a more accurate representation of load dynamics (i.e., composite load model).

5 Conclusions

The main findings and conclusions from the work completed are as follows:

1. The bench testing demonstrates diversity in inverter response to the same disturbance. This difference can, consequently, impact the modelling and aggregation of DERs for bulk power system (BPS) studies. *This is shown in Chapter 2.* The bench testing has also provided possible explanations for unwarranted disconnection of large numbers of inverters during grid disturbances.
2. A set of voltage and frequency disturbances has been analysed using PMU and high-speed PQM data. Possible DER trip events have been observed. More information from the monitored feeders, e.g., load composition, voltage control strategy, etc will assist in confirming the proposed mechanisms. One of the main challenges is to discernment between the voltage and frequency dependency of the traditional loads and the response of DERs to voltage and frequency disturbances. Hence, in addition to the DER modelling, it is very important to present dynamic of the load accurately by considering correct load composition. See *Chapter 3 for details.*
3. This subtask utilises the DER_A model that was recently developed by the Western Electricity Coordinating Council (WECC) to represent the DERs [1]. This model mimics the aggregated behaviour of inverter-based DERs on a load bus for voltage and frequency disturbances. The model is generic and can be parameterised for different DERs' settings. Based on the findings from Task 1 and Task 2, as well as the requirements set at AS4777.3-2005 and AS4777.2-2015, the parameters are tuned for voltage and frequency disturbance. See *Chapter 4 for more details.*

6 References

- [1] P. Pourbeik, K. Clark, J. Boemer and et al, *Proposal for DER_A model*, WECC, 2018.
- [2] J. V. Milanović, J. Matevosyan and e. al, "Modelling and aggregation of loads in flexible power networks," CIGRE_Working_Group_C4.605, 2014.
- [3] AS/NZS, *AS/NZS 4777.2:2015 Grid connection of energy systems via inverters*, 2015.
- [4] AS/NZS, *AS 4777 - 2005 Grid Connection of Energy Systems via Inverters*, 2005.
- [5] J. v. Appen, M. Braun, T. Stetz, K. Diwold and D. Geibel, "Time in the Sun: the Challenge of High PV Penetration in the German Electric Grid"," *IEEE Power and Energy Magazine*, vol. 11, no. 2, pp. 55 - 64, March/April 2013.
- [6] AEMO, "Response of existing PV inverters to frequency disturbances," AEMO, April 2016.
- [7] WECC, "WECC Dynamic Composite Load Model (CMPLDW) Specifications," 2015.
- [8] NERC, "Reliability Guideline – Developing Load Model Composition Data," 2017.
- [9] NERC, "Technical Reference Document – Dynamic Load Modelling," 2016.

Contact: John Fletcher

Email: john.fletcher@unsw.edu.au

END